**University of Crete**

**School of Medicine**

**Master's Graduate Program**

**''Neurosciences''**

*Master thesis*

# Involvement of macroautophagy in nigrostriatal axonal degeneration induced by inhibition of Chaperone-Mediated Autophagy

Fouka Maria

**Thesis advisory committee:**

Leonidas Stefanis, MD, PhD, Professor of Neurology and Neurobiology (Supervisor)

Domna Karagogeos, PhD, Professor of Molecular Biology - Developmental Biology

Vasiliki Nikoletopoulou, PhD, Professor of Neurobiology and Metabolism

*Crete, 2019*

# Table of Contents


**A. Introduction**.....4

A.1 What is autophagy?.....4

A.2 Macroautophagy machinery.....5

A.3 Physiological roles of autophagy.....8

A.4 Autophagy and neurodegenerative diseases.....9

A.5 Chaperone Mediated Autophagy (CMA) .....12

A.6 Physiological roles of CMA.....14

A.7 CMA impairment and neurodegeneration.....16

A.8 CMA and Parkinson's disease: Lessons from α-Synuclein.....17

A.9 Crosstalk between Macroautophagy and CMA.....22

**B. Aim of the Study**.....24

**C. Materials and Methods**.....25

C.1 Animals.....25

C.2 Surgical Procedures .....25

C.3 Perfusion, fixation and sectioning of rat brains.....25

C.4 Immunofluorescence.....26

C.5 Automated image analysis.....26

C.6 DAB immunostaining.....27

C.7 Densitometry.....27

C.8 Electron microscopy.....27

C.9 Preparation of Synaptosomes.....28

C.10 Western blotting.....28

**D. Results**……31

D.1 Efficient transduction of the rat nigrostriatal pathway with rAAVs……31

D.2 Downregulation of LAMP2A in transduced dopaminergic neurons……...32

D.3 CMA impairment is accompanied by increased LC3 levels and decreased SQSTM1/p62 levels within transduced degenerating nigral neurons……..33

D.4 CMA deficiency results in accumulation of AVs within $GFP^+$ transduced degenerating nigral neurons, at 3 weeks post injection……36

D.5 LAMP2A down-regulation is accompanied by accumulation of AVs in the striatum as early as 2 weeks post-injection……37

D.6 LAMP2A down-regulation results in accumulation of early AVs in the synaptic terminals, at 3 weeks post-injection ……39

D.7 CMA deficiency is accompanied by increased ULK1 levels within $GFP^+$ transduced nigral neurons, at 3 weeks post-injection……42

D.8 LAMP2A down-regulation leads to impaired dopaminergic synaptic integrity, which is detected prior to nigral cell degeneration……..43

D.9 Increased astrogliosis and microgliosis throughout the nigrostriatal axis in LAMP2A-deficient rats, at 3 weeks post-injection……45

**E. Discussion**……49

**F. References**……57

**G. List of Abbreviations**……69

# Abstract

Chaperone-mediated autophagy (CMA) is one of the main autophagic proteolytic pathways involving the selective targeting of cytosolic proteins to the lysosomes. It is widely believed that dysfunction of the CMA pathway is important in the pathogenesis of Parkinson's disease (PD). In order to model this, we have recently generated a novel rat model, in which downregulation of CMA within the nigra, via AAV-shRNA-mediated targeting of endogenous Lamp2a, the rate-limiting step in the CMA pathway, leads to loss of striatal dopamine, nigral neuron degeneration, and accumulation of alpha-synuclein, 8 weeks post injection, thus mimicking aspects of PD. In this system, we have observed a marked accumulation of autophagic vacuoles and biochemical indices suggestive of enhanced productive macroautophagy in the nigral cell bodies of dopaminergic neurons. In view of these features, aim of the current study was to assess the contribution of macroautophagy to the dopaminergic axonal degeneration that precedes nigral cell death, evoked by inhibition of the Chaperone-mediated autophagy (CMA) pathway.

In order to inhibit CMA, we have stereotaxically injected adeno-associated viruses expressing shRNAs targeting LAMP2A receptor or scrambled shRNAs in the rat substantia nigra (SN). At 2 and 3 weeks post-injection, we examined indices of macroautophagy induction and the formation of autophagic vacuoles (AVs) in the nigrostriatal axis by Confocal and Electron Microscopy. The integrity of the nigrostriatal projections and the astro- and micro-gliosis in both striatum and SN at these time-points were also assessed by Confocal Microcscopy.

LAMP2A down-regulation was accompanied by abnormal accumulation of AVs at synaptic nerve terminals, prior to dopaminergic degeneration at 3 weeks post-injection. At this early time point, the levels of Bassoon, a negative regulator of autophagy and a marker for the active synaptic zone, were decreased, whereas levels of ULK-1 were increased. Increased astro- and micro-gliosis was observed in both SN and striatum.

Our data suggest that uncontrolled induction of macroautophagy may, at least in part, be responsible for the nigrostriatal terminal degeneration that occurs early in this model, well before cell soma degeneration. Further, our results provide the first *in vivo* evidence that ULK-1 is a CMA substrate and may act as a link between CMA and macroautophagy. Therefore, down-regulation of macroautophagy may represent a promising target to reverse the damage and rescue the deteriorating dopaminergic neurons.

# Περίληψη

Η αυτοφαγία διαμεσολαβούμενη από σαπερόνες (CMA) αποτελεί μία από τις κύριες αυτοφαγικές πρωτεολυτικές οδούς που εμπλέκονται στην επιλεκτική στόχευση κυτοσολικών πρωτεϊνών στα λυσοσώματα. Πιστεύεται ευρέως ότι η δυσλειτουργία του CMA μονοπατιού είναι σημαντική στην παθογένεση της νόσου του Πάρκινσον. Για να το μοντελοποιήσουμε αυτό, πρόσφατα δημιουργήσαμε ένα νέο μοντέλο επίμυος, στο οποίο η μειωμένη ενεργότητα του CMA εντός της μέλαινας ουσίας, μέσω της σίγασης του ειδικού υποδοχέα του μονοπατιού LAMP2A, οδήγησε σε μείωση των επιπέδων της ντοπαμίνης στο ραβδωτό σώμα, εκφυλισμό των ντοπαμινεργικών νευρώνων και συσσώρευση της πρωτεΐνης α-συνουκλεΐνης, 8 εβδομάδες μετά την έγχυση των ιών, μιμούμενη έτσι βασικά χαρακτηριστικά της νόσου του Πάρκινσον. Σε αυτό το σύστημα, παρατηρήσαμε μία σημαντική αύξηση αυτοφαγικών κυστιδίων και βιοχημικών δεικτών που υποδηλώνουν την παρουσία αυξημένης παραγωγικής μακροαυτοφαγίας στα σώματα των ντοπαμινεργικών νευρώνων. Λόγω αυτών των χαρακτηριστικών, στόχος της παρούσας μελέτης ήταν να εκτιμηθεί η συμβολή της μακροαυτοφαγίας στον ντοπαμινεργικό νευραξονικό εκφυλισμό που προηγείται του θανάτου των κυτταρικών σωμάτων, ο οποίος προκαλείται έπειτα από την αναστολή του CMA μονοπατιού.

Προκειμένου να ανασταλεί το CMA, εγχύθηκαν στερεοτοξικά αδενο-συσχετιζόμενοι ιοί που εκφράζουν shRNAs που στοχεύουν τον υποδοχέα LAMP2A ή μη κωδικά shRNAs στη μέλαινα ουσία επίμυων. Στις 2 και 3 εβδομάδες μετά την έγχυση, εξετάσαμε δείκτες επαγωγής μακροαυτοφαγίας και σχηματισμού αυτοφαγικών κυστιδίων (AVs) στο μελανοραβδωτό άξονα με ηλεκτρονική μικροσκοπία και μικροσκοπια φθορισμού. Η ακεραιότητα των ντοπαμινεργικών αξόνων και η αστρο- και μικρο-γλοίωση τόσο στο ραβδωτό όσο και στη μέλαινα ουσία, σε αυτά τα χρονικά σημεία, αξιολογήθηκαν επίσης με μικροσκοπία φθορισμού.

Η σίγηση του υποδοχέα LAMP2A συνοδεύτηκε από ανώμαλη συσσώρευση των AVs στις συναπτικές απολήξεις, πριν από τον ντοπαμινεργικό εκφυλισμό στις 3 εβδομάδες μετά την έγχυση. Σε αυτό το αρχικό χρονικό σημείο, τα επίπεδα του Bassoon, ενός αρνητικού ρυθμιστή της αυτοφαγίας και δείκτη της συναπτικής ενεργότητας μειώθηκαν, ενώ τα επίπεδα της πρωτείνης ULK-1, που ρυθμίζει τη μακροαυτοφαγία, αυξήθηκαν. Αυξημένη αστρο- και μικρο-γλοίωση παρατηρήθηκε τόσο στη μέλαινα ουσία όσο και στο ραβδωτό σώμα.

Τα δεδομένα μας υποδεικνύουν ότι η ανεξέλεγκτη επαγωγή της μακροαυτοφαγίας μπορεί, τουλάχιστον εν μέρει, να είναι υπεύθυνη για τον εκφυλισμό των ντοπαμινεργικών απολήξεων που εμφανίζεται νωρίς σε αυτό το μοντέλο, πολύ πριν από τον εκφυλισμό του κυτταρικού σώματος. Περαιτέρω, τα αποτελέσματά μας παρέχουν τις πρώτες in vivo αποδείξεις ότι το ULK-1 αποτελεί υπόστρωμα του CMA μονοπατιού και μπορεί να δρά ως σύνδεσμος μεταξύ του CMA και της

μακροαυτοφαγίας. Επομένως, η μείωση της μακροαυτοφαγίας μπορεί να αποτελέσει έναν πολλά υποσχόμενο στόχο για να αναστρέψει τη βλάβη και να διασώσει τους ντοπαμινεργικούς νευρώνες.

# A. Introduction

### *A.1 What is autophagy?*

Cellular homeostasis requires a proper balance between protein synthesis and degradation. Eukaryotic cells have two major intracellular proteolytic systems, the lysosome and the proteasome. The proteasome is the primary selective degradation system; it generally recognizes only ubiquitinated substrates, which are primarily short-lived proteins. Degradation via the lysosome is more complex. Extracellular material and plasma membrane proteins can be delivered to lysosomes for degradation via the endocytic pathway. Furthermore, cytosolic components and organelles can also be delivered to the lysosome through the autophagy machinery.

Autophagy is an evolutionarily conserved catabolic self-degradation process by which cells degrade and recycle their intracellular components. Three distinct types of autophagy have been identified: macroautophagy, microautophagy and endosomal microautophagy and chaperone-mediated autophagy (CMA) **(Fig. 1)**. These types vary from each other depending on the inducing signals and temporal aspects of induction, type of cargo and mechanism of sequestration (Klionsky et al. 2016).

Macroautophagy is thought to be the major type of autophagy, and it has been studied most extensively compared to microautophagy and CMA. This pathway is conserved from yeast to mammals and is mediated by a special organelle termed the autophagosome (Nakatogawa et al. 2009). A second autophagic pathway, microautophagy, is a specialized form of autophagy in which cytoplasmic proteins and organelles engulfed by lysosomes or the vacuole (in yeast) via direct invagination of the lysosomal membrane in either selective or non-selective manner (Marzella et al. 1981; Galluzzi et al. 2017). Recent studies have shown that microautophagy actually occurs in mammals, but in late endosomes/multivesicular bodies (LE/MVB) instead of lysosomes (Sahu et al. 2011). This process termed endosomal-microautophagy (eMI), contributes to the bulk degradation of proteins present in cytosol trapped in vesicles forming at the LE membrane. This process was initially thought to be non-selective, but recent reports showed that some cytosolic proteins can be delivered to late endosomes by HSC70, which may represent a form of selective microautophagy (Sahu et al., 2011; Uytterhoeven et al., 2015). The HSC70 chaperone is also involved in CMA, a selective degradation process. The chaperone HSC70 and its co-chaperones recognize cytosolic substrate proteins bearing the loose pentapeptide motif, KFERQ or a biochemically related one (Chiang et al., 1989, Dice, 1990) and associate with the lysosomal membrane protein LAMP2A, resulting in client protein translocation into the lysosome (Kaushik and Cuervo, 2012).

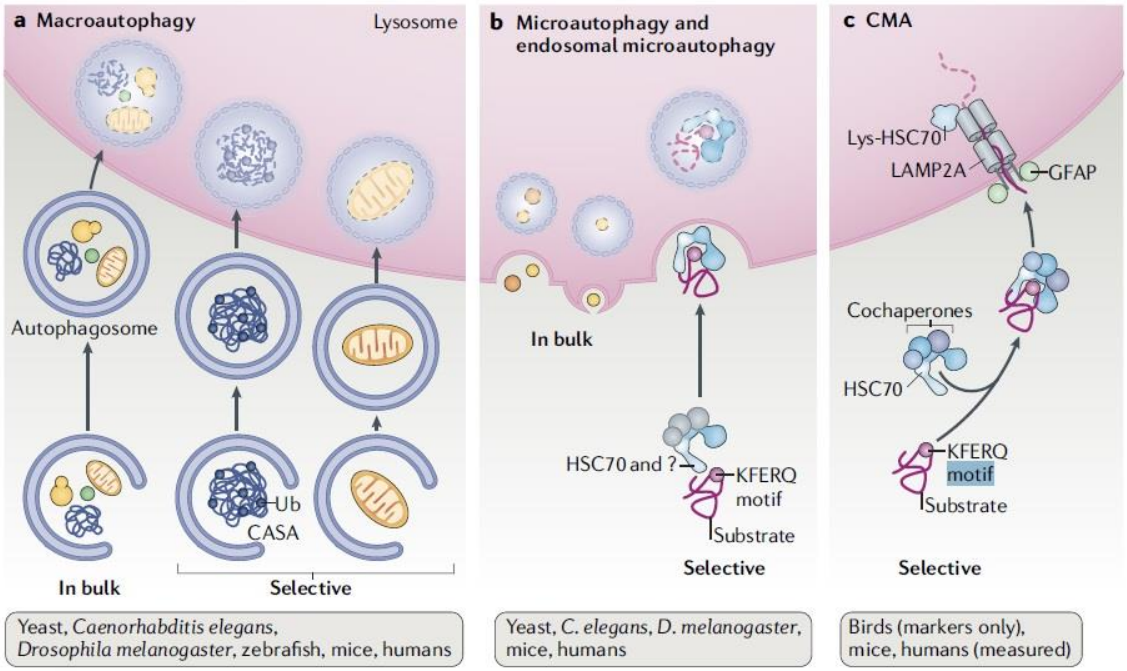


***Figure 1. Autophagic pathways in mammals.*** *Three major autophagy pathways have been described; macroautophagy, microautophagy and endosomal microautophagy and chaperone-mediated autophagy (CMA). All types are involved in degradation of intracellular components in order to synthesize proteins, produce energy and contribute to gluconeogenesis* ***(adapted from Kaushik et al. 2018).***

### *A.2 Macroautophagy Machinery*

Autophagy is regulated by the autophagy-related genes (Atg) that have been discovered in the yeast Saccharomyce cerevisiae. From these 31 genes, 15 are mainly required for the autophagic machinery, and only 11 of them have unambiguous orthologous in mammals. Most of these "core" Atg's mediate the autophagosome formation (Klionsky et al. 2003; Nakatogawa et al. 2009). The process of autophagosome formation is orchestrated by two major steps: nucleation and elongation of the isolation membrane. The nucleation step is processed by the ULK/Atg1 kinase complex, the autophagy-specific PI3-kinase complex and PI(3)P effectors and their related proteins, whereas the elongation step is mediated by the Atg12- and LC3/Atg8-conjugation systems. At the final step, the autophagosome fuses with the lysosome leading to the degradation of the cargo (Klionsky et al. 2000).

More specifically, there are five highly conserved steps in autophagy (**Fig. 2**):

1. Initiation

2. Vesicle nucleation

3. Vesicle elongation

4. Maturation, Axonal Transport (neurons) and Fusion with the lysosome

5. Degradation

The initiation of the phagophore formation, which is, a double membrane organelle that encloses and isolates the cytoplasmic components, begins when the ULK kinase complex is activated, and involves the translocation of the ULK complex at a distinguished location on the endoplasmic reticulum (ER), marked by the ATG9 protein. The ULK1 (unc-51-like kinase 1) (Atg1 in yeast) complex senses the nutrient status of the cell to initiate or terminate autophagy. Autophagosomes are generated on, or in close proximity, to the ER (Mizushima et al., 2011, Tooze and Yoshimori, 2010). However, it remains unclear whether the ER membrane is directly used for autophagosome formation. Recent studies suggest that additional membranes derived from the Golgi complex, the mitochondria, and the plasma membrane also contribute to autophagosome formation (Hailey et al. 2010, Mizushima et al. 2011, Ravikumar et al. 2010, Tooze and Yoshimori 2010).

ULK1 is negatively regulated by the mammalian target of rapamycin complex 1 (mTORC1), in a nutrient-dependent manner. Upon autophagy induction, this complex consisting of ULK1, Atg13, FIP200, and Atg101 is activated in an adenosine monophosphate-activated protein kinase (AMPK)-dependent manner and translocates to early autophagic structures (Kim et al. 2011). The active ATG1 complex is translocated to the ER and activates the class III phosphatidylinositol (PtdIns) 3-kinase complex (including Ambra1, Beclin 1, Atg14(L)/barkor, Vps15 and Vps34). Subsequently, the activation of PtdIns3 complex signals triggers vesicle nucleation.

The expansion of the phagophore and, ultimately, the formation of the autophagosome, are being mediated by two ubiquitin-like ATG conjugation pathways, the ATG5-ATG12 and the LC3/Atg8 complexes. The proteins with ubiquitin-like proteins (UBLs) activity, ATG12 and ATG8, undergo a cascade of conjugation with different ATG interactors. In mammals, there are seven Atg8 orthologues; MAP1LC3A/B/C, GABARAP and GABARAPL1/2/3 (all of which are hereafter referred to as LC3). LC3 is widely used as a marker for the microscopic detection of isolation membranes and autophagosomes. After synthesis, LC3 is post-translationally modified by the ATG4 protein, a cysteine protease, and becomes LC3-I, which has a

glycine residue at the C-terminal end. Once autophagy is induced, ATG7 activates LC3 and transfers it to ATG3 (E2-like enzyme). LC3-I is subsequently conjugated with phosphatidylethanolamine (PE) to become LC3-II by an ubiquitination-like enzymatic reaction. In contrast to the cytoplasmic localization of LC3-I, LC3-II associates with both the outer and inner membranes of the autophagosome. The PE-LC3 is integrated in the pre-autophagosome and is involved in the generation of mature autophagosomes and in cargo recognition (Fullgrabe et al., 2014). PE-conjugated LC3 (LC3-II) and unconjugated LC3 (LC3-I) can be distinguished separately by immunoblot analysis, and the amount of LC3-II is widely used for the quantification of autophagic activity (Kabeya et al., 2000).

It is believed that the expanding autophagosomes engulf bulk cytoplasmic contents in a non-specific manner. However, this process may also be selective through cargo receptors delivering ubiquitinated substrates for autophagic degradation. Such a receptor is the mammalian protein p62/sequestosome 1 (SQSTM1), which contains a C-terminal ubiquitin-associated (UBA) domain that binds ubiquitin, and a short LC3-interacting region (LIR) sequence, that allows LC3 interaction (Pankiv et al. 2007). On the other hand, p62 is itself an autophagy-substrate and the selective recognition and degradation of p62 through autophagy were demonstrated by its accumulation in autophagy deficient cells (Wang et al. 2006). The protein levels of LC3II and p62 are being widely used as an index of autophagic flux, since their levels correlate directly with the rate of autophagic activity.

Regarding neuronal cells, it is generally believed that autophagosome biogenesis events are enriched distally but are infrequent in dendrites, the soma or the mid axon (Maday et al. 2015). De novo formation of autophagosomes has been detected in cell bodies of primary cortical neurons (Lee et al. 2011). However, it remains unclear whether autophagosome biogenesis occurs along the axons. Once formed, the autophagosomes in distal axons undergo robust retrograde transport towards the soma, where the lysosomes are located, in a dynein-dependent manner (Cheng et al. 2015; Hollenbeck 1993; Lee et al. 2011; Maday et al. 2012; Maday and Holzbaur 2014). As autophagosomes travel along the axon, they mature into degradative organelles (Lee et al. 2011; Maday et al. 2012; Wang et al. 2015). Autophagosomes along the mid-axon are positive for the late endosome/lysosome marker LAMP1, suggesting that exit from the distal axon is accompanied by fusion with late endosomes/lysosomes (Maday etal. 2012). In the final step, the autophagosome fuses with the lysosome to become autolysosome, where the degradation of the contained materials is mediated by the lysosomal hydrolases (Dice 2000). The macromolecules are digested to their monomeric units, and released to the cytosol for reuse. However, this process has to be further explored; especially, the process of the autophagic recycling of carbohydrates and lipids remains extremely unknown.

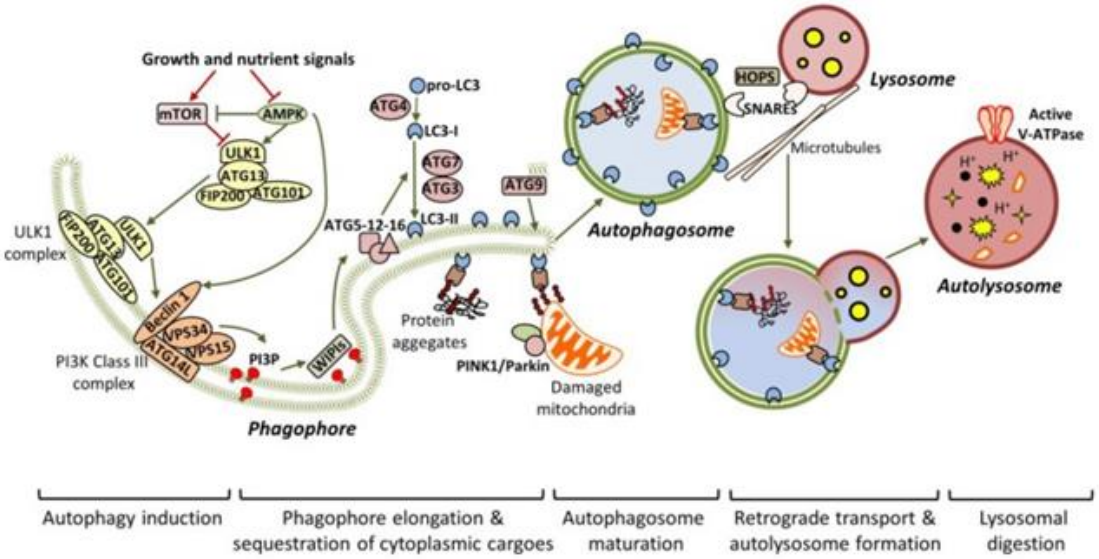


***Figure 2: Schematic representation of the macroautophagic pathway in mammalian cells.*** *The core autophagy proteins which constitute the molecular pathway of autophagy are illustrated with their associated autophagy membrane compartments. The 5 major steps in the autophagic pathway are shown (adapted from Metaxakis et al. 2018).*

### *A.3 Physiological roles of autophagy*

Basal autophagy occurs constantly within the majority of mammalian cells at low levels; however a wide range of stimuli can upregulate autophagy highlighting the importance of this pathway in cellular survival and homeostasis. Traditionally, autophagy was thought to be primarily an adaptive response to starvation, as it enables recycling of macromolecules providing the cells with the necessary amino acids (Mizushima et al. 2004). However in the last years, autophagy has emerged as a multifunctional pathway involved in intracellular quality control, development, cell death, tumor suppression and anti-aging.

A principal function of autophagy is the elimination of cytoplasmic contents. Research during the last 15 years has revealed that autophagy contributes to intracellular homeostasis in non-starved cells by degrading cargo material such as aggregate-prone proteins, including those causing many neurodegenerative conditions (aggrephagy), damaged mitochondria (mitophagy), excess peroxisomes (pexophagy), and invading pathogens (xenophagy) (Stolz et al. 2014). In the classical example, aggregates of aberrantly folded proteins are tagged with ubiquitin chains that are recognized by ubiquitin-binding domain-containing receptors, such as SQSTM1/p62 (Bjørkøy et al. 2005), neighbor of BRCA1 gene 1 (NBR1) (Kirkin et al. 2009), optineurin (OPTN) (Wild

et al. 2011), TOLL-interacting protein (TOLLIP) (Lu et al. 2014) and others. These receptors also contain LC3-interacting region (LIR) motifs in their sequences that can recognize the key autophagosome-associated protein, LC3. Thus, these receptors link the autophagy machinery to ubiquitinated protein substrates for subsequent lysosomal degradation (Bjørkøy et al. 2005; Pankiv et al. 2007). Besides neuronal homeostasis, autophagy has also been shown to intersect with many of the pathways related to synaptic plasticity and participate in processes that underlie the continuous remodeling of the neuronal terminals (Komatsu et al. 2007; Wang et al. 2006; Nikoletopoulou et al. 2017), suggesting that it also contributes to neuronal function. At the Drosophila neuromuscular junction, high-frequency stimulation results in a rapid increase in Atg8 (LC3) puncta formation at presynaptic terminals (Soukup et al., 2016; Vanhauwaert et al., 2017), whereas in rat hippocampal pyramidal neurons, neuronal stimulation induces autophagosome formation, which promotes presynaptic AMPA receptor degradation (Shehata et al., 2012). Autophagy has also been implicated in the degradation of postsynaptic receptors such as inhibitory $GABA_A$ receptors and AMPA receptors, thereby inducing synaptic long-term depression (Rowland et al., 2006; Shehata et al., 2012). These reports proposed autophagy as a new player in the synaptic plasticity.

Based on the increasing evidence for the physiological importance of autophagy in neuronal homeostasis and function, it seems unsurprising that alterations in the autophagic machinery are intimately linked to different brain diseases, including a growing number of neurological disorders, such as Alzheimer's Disease (AD), Parkinson's Disease (PD), Huntington's Disease (HD) and Amyotrophic Lateral Sclerosis (ALS).

### *A.4 Autophagy and neurodegenerative diseases*

The turnover of proteins has been the focus of attention across neurodegenerative diseases, given that many, if not all, of these diseases, show characteristic protein aggregation as the key hallmark of their cellular pathology. Although the underlying mechanisms responsible for the formation of the proteinaceous inclusions remains largely unknown, a common link is the fact these aggregate-prone proteins are substrates for autophagic degradation (Menzies et al., 2015a; Ravikumar et al., 2002). Different findings in recent years have aided to consolidate a connection between macroautophagy and neurodegenerative disorders and propelled the current interest in this topic.

As post-mitotic cells, neurons cannot dilute out aggregated proteins and damaged organelles in the cytoplasm by cell division. Thus, neurons are particularly dependent on a proper cellular protein-quality-control system to eliminate these toxic materials

and maintain their own homeostasis. An increasing body of evidence during the last years indicates that in neurons, basal autophagy is essential for maintenance of local homeostasis of axonal compartment and protection against axonal degeneration. This protective effect appears to be related to the elimination of damaged mitochondria and toxic protein aggregates. By contrast, dysregulation of autophagy leads to accumulation of abnormal proteins and eventually to neuronal dysfunction and impaired axonal transport (Millecamps and Julien 2013), events that may eventually result in or contribute to axonal degeneration and subsequent neuronal death. In many neurodegenerative diseases, such as PD, AD and ALS, the axon is the first damaged neuronal compartment, an event that often occurs many years before the death of cell body becomes evident (Tagliaferro et al. 2016). Moreover, it has been reported that autophagosome-like vacuoles are present in the dysfunctional or degenerating axons, which suggest that altered autophagy may mediate the subsequent neuronal death (Rubinsztein et al. 2005; Maday 2016). These observations link altered autophagy and axonopathy, which is one of the underlying mechanisms leading to neurodegeneration (Coleman and Perry 2002).

The strongest evidence for an active role of autophagy in maintaining neuronal homeostasis arose from the generation of mutant mice lacking key autophagy genes. More particularly, it has been shown that *in vivo* depletion of the Atg5 gene in the neural lineage provokes neuronal cell loss, progressive motor deficit and accumulation of protein aggregates and inclusion bodies in neurons (Hara et al. 2006). In the same manner, mice with conditional deletion of Atg7 in the neural lineage display cell loss in the cerebral and cerebellar cortices, motor impairments and inclusion formation. These mice also show axonal swelling and die at around 28 weeks (Komatsu et al. 2007). Friedman et al. demonstrated that dopaminergic (DA) neuron-specific autophagy deficiency leads to the restrictive presynaptic accumulation of α-synuclein in the dorsal striatum and delayed neurodegeneration, suggesting that impaired autophagy plays a role in PD pathogenesis (Friedman et al. 2012). More recently, Sato and colleagues also generated a DA cell-specific Atg7 conditional knockout mice resulting in Lewy pathology and motor dysfunction associated with aging (Sato et al. 2018). These results suggest that the continuous clearance of diffuse cytosolic proteins through basal autophagy is important for preventing the accumulation of abnormal proteins, which can disrupt neural function and ultimately lead to neurodegeneration. On the other hand, Hu et al. provide evidence that Atg5 overexpression can exert protection against MPTP-induced Parkinsonism, by restoring levels of DA in zebrafish (Hu et al. 2017). Moreover, activation of mTOR-dependent macroautophagy has been shown to inhibit the accumulation of α-synuclein (Sheng et al., 2017).

In addition, it has been shown that chronic macroautophagy deficiency in DA neurons results in abnormally large dopaminergic axonal profiles and increased

neurotransmitter release in response to stimuli, strengthening the view that autophagy plays a crucial role in the presynaptic terminals and synaptic activity in general (Hernandez et al. 2012). It is believed, therefore, that autophagy acts as a brake of presynaptic activity, regulating the kinetics of DA release (Shen et al. 2015).

Despite the well-established neuroprotective role of autophagy in most cases of neuronal injury, excessive autophagy has also been proposed to contribute to neurodegeneration. For example, inhibition, rather than stimulation, of macroautophagy promotes neuronal survival in some pathological conditions displaying increased neuronal autophagic vacuoles. Yang et.al provided evidence that autophagy mediates neurite retraction after nerve growth factor deprivation in cervical ganglion neurons (Yang et al, 2007). In this study, autophagic degeneration occurs prior to cell death, suggesting that autophagy plays a role in neurite degeneration independent of cell death. Interestingly, molecular and pharmacological inhibition of autophagy efficiently suppressed axonal and dendritic degeneration in this model (Yang 2007). We have also previously shown that in rat primary cortical neurons and in human differentiated DA SH-SY5Y cells, CMA inhibition conferred by aberrant alpha-synuclein overexpression lad to a compensatory induction of the process of macroautophagy and cell death. Interestingly, pharmacological and molecular macroautophagy inhibition exerted a protective effect in both models, further supporting a neurotoxic role of excessive macroautophagy induction (Xilouri et al. 2009). Furthermore, in a model of excitotoxic neurodegeneration, excessive induction of autophagy was found to be associated with axonal dystrophy, even in the absence of an altered rate of degradation. The authors proposed that, particularly in axons, a common pathway exists downstream of specific disease mechanisms, which triggers the induction of autophagy before the onset of neuronal death (Wang et al. 2006). Autophagic stress has also been implicated in neurons exposed to methamphetamine, which causes neuritic dystrophy in the absence of cell death, and elevated autophagic activity was found to be associated with decreased dopaminergic neurotransmission (Larsen et al. 2002). Still, the question of whether or not there is “excessive” autophagy mediating “autophagic cell death” remains one of the most controversial issues in the field.

### *A.5 Chaperone Mediated Autophagy (CMA)*

CMA, which is responsible for the degradation of selected soluble proteins, differs from the other two types of autophagy, on the mechanism mediating the cargo selection and the mode of cargo delivery to the lysosomal lumen for degradation. It is a selective form of autophagy in which cytosolic proteins containing a specific

targeting motif in their amino acid sequence are targeted to the lysosome for degradation. The delivery of substrate-proteins does not require the formation of intermediate vesicles, membrane fusion, or membrane deformity of any type. Instead, the substrates are translocated from the cytosol directly into the lysosomal lumen across the membrane in a process mediated by a translocation protein complex that requires substrate unfolding.

The selective process of CMA can be divided into four distinct steps (**Fig. 3**):

(a) Substrate recognition and targeting to the lysosomes;

(b) Substrate binding to the lysosomal receptor and unfolding;

(c) Substrate translocation through the lysosomal membrane and

(d) Substrate degradation in the lysosomal lumen

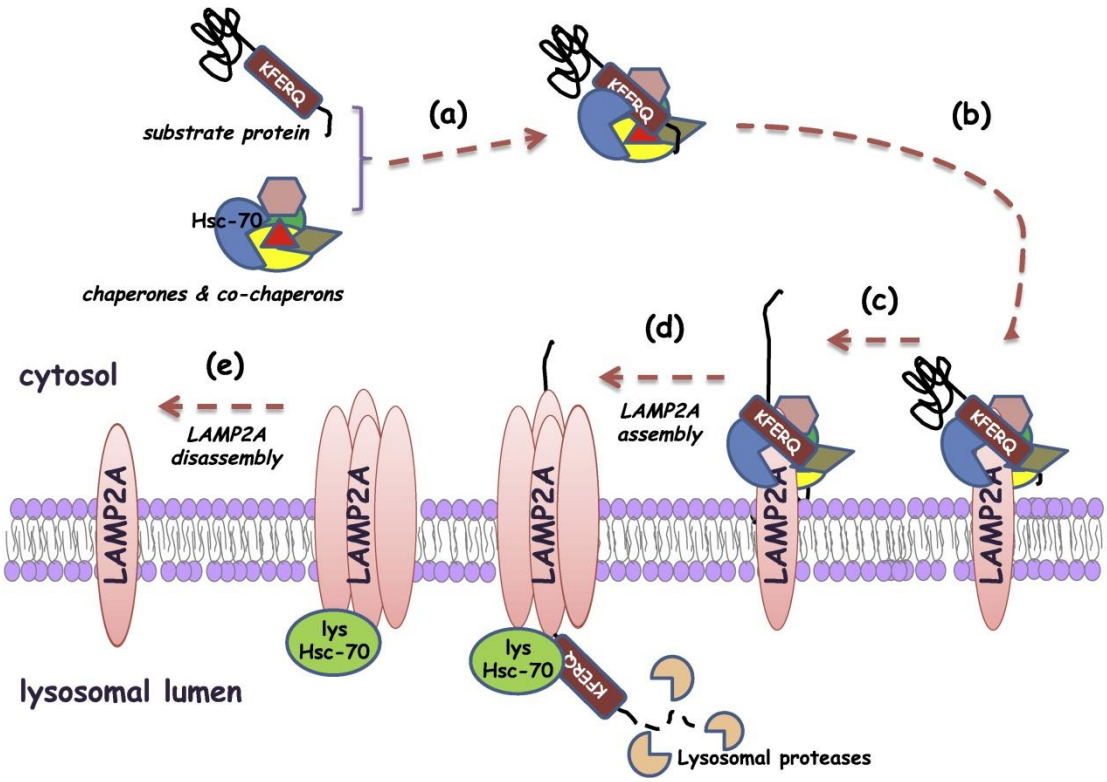


***Figure 3. Schematic representation of the CMA pathway machinery.*** The selective process of CMA starts with the recognition of a substrate protein bearing a KFERQ-like motif by a chaperone/co-chaperone complex in the cytosol (a). This complex transfers the protein to the surface of the lysosomal membrane, where the binding to the cytosolic tail of the LAMP2A receptor takes place (b). This binding promotes LAMP2A multimerization and substrate unfolding with the aid of the lysosomal HSC-70 (c), thus promoting the direct translocation of the protein across the lysosomal membrane and

its subsequent degradation by the lysosomal proteases (d). Following substrate translocation, lys-HSC70 enables disassembly of the LAMP2A complex (e), which is then available for the binding of other substrates (adapted from Xilouri et al. 2016).

All CMA substrates are soluble cytosolic proteins bearing the loose pentapeptide motif KFERQ, or a biochemically related one (Dice et al. 1986; Chiang and Dice (1988). During the first step, CMA substrate proteins are targeted for lysosomal degradation by the heat-shock cognate protein of 70 kDa (HSC70, a cytosolic member of the HSP70 chaperone family) (Chiang et al. 1989, Dice 1990). The interaction between the substrate protein and HSC70 is being modulated by the HSC70 co-chaperones, such as HSP40, HSP90, Hip, Hop, and Bag (Agarraberes and Dice 2001). Athough almost 30% of cytosolic proteins contain a KFERQ-like motif, few of them have been tested for their actual degradation by this pathway (Wing et al. 1991). Since the CMA motif is based on the charge of the amino acids, it is likely that other proteins could acquire the loose pentapeptide motif targeting them to CMA after post-translational modifications, such as phosphorylation or acetylation in the case of Huntingtin (Thompson et al. 2009). Substrate proteins are required to be unfolded before translocation into the lysosomal lumen. HSC70 and the co-chaperons not only target the CMA substrate to the lysosomal membrane, where it can interact with the CMA receptor, but likely also participate in the unfolding step required before the substrate translocation across the lysosomal membrane (Agarraberes and Dice 2001).

The second step of the pathway involves the translocation of the HSC70-co-chaperones / substrate complex to the level of the lysosomal membrane, where the interaction with the cytosolic tail of the single-span membrane protein lysosome-associated membrane protein type 2A (LAMP2A) takes place. HSC70 and the substrate can bind the LAMP2A tail at the same time, suggesting that substrate recognition and targeting are coupled processes; however, the KFERQ-like motif in the substrate is not required for LAMP2A binding (Cuervo and Dice, 1996). LAMP2A is one of three isoforms of the *LAMP2* gene, encoded through alternative splicing and the only isoform required for CMA. All *LAMP2* isoforms (LAMP2A, LAMP2B, LAMP2C) are lysosomal transmembrane proteins, which share a common highly N-glycosylated lumenal region, but different transmembrane domain and cytosolic tail (Gough NR et al. 1995). LAMP2A is the rate-limiting step for the whole CMA process. Consequently, changes in the levels and dynamics of LAMP2A at the lysosomal membrane regulate CMA activity. LAMP2A exists as a monomer at the lysosomal membrane. The binding of substrates to LAMP2A monomers triggers the multimerization of LAMP2A into a multimeric protein complex that acts as the active translocation complex through which the substrate proteins are threaded into the lysosomal lumen and degraded. The stability of LAMP2A into a multimeric complex at the lysosomal membrane and

the subsequent translocation of the substrate protein require the presence of a lysosomal form of HSC70 (lys-HSC70) and co-chaperones in the lysosomal lumen.

The final step is the rapid proteolysis of the substrate by residual lysosomal proteases inside the lysosomal lumen. Once the substrate protein is translocated into the lumen, LAMP2A disassembles from this multimeric complex, which is then accessible to bind other substrates, a process that only takes place when free monomers of the receptor are available (Bandyopadhyay et al. 2010) Alternatively, LAMP2A can be displaced into the lysosomal lumen, where it does not participate in CMA and can be degraded by cathepsin A (Cuervo et al. 2003).

### *A.6 Physiological roles of CMA*

CMA operates at basal conditions in most mammalian cell models analyzed so far, but its activation is often triggered by various stressors, such as trophic deprivation (Cuervo et al. 1995), oxidative stress (Kiffin R et al. 2004) or protein denaturation (Cuervo et al. 1999). Under these conditions, CMA responds with compensatory mechanisms including increased LAMP2A transcription, decreased LAMP2A clearance within the lysosomal lumen, or increased abundance of luminal lys-HSC70.

Research during the last 10 years has highlighted the contribution of CMA to the maintenance of energetic cellular balance and cellular quality control. Under conditions of nutrient deprivation, CMA is activated in order to degrade and recycle intracellular components, providing energy and building blocks. In the classical paradigm of nutritional starvation, the cells respond immediately by activating macroautophagy. If the starvation state is prolonged for more than 10 hours, then cells activate CMA. The selectivity of CMA for individual cytosolic proteins allows cells to degrade only those proteins that might not be required under these starvation conditions in order to generate amino acids for the synthesis of essential proteins.

The other major utility of CMA is the specific elimination of abnormal or damaged proteins. Although CMA cannot degrade proteins as soon as they aggregate, it is part of the first line of defense against protein aggregation by mediating the degradation of individual proteins after damage or partial unfolding (Cuervo 2004, Martinez-Vicente et al. 2008). This is of particular importance in conditions that are related to protein damage, such as oxidative stress or toxic agents. Supporting this idea, it has been reported that CMA is upregulated during oxidative stress (Kiffin et al., 2004) or exposure to toxic compounds (Cuervo et al., 1999) and cells deficient in CMA are more susceptible to oxidative agents (Massey et al., 2006), whereas *in vitro* as well as *in vivo* upregulation of CMA is accompanied by reduced levels of oxidized and aggregated proteins improving cellular resistance to proteotoxicity (Anguiano et al.

2013). However, the physiological role of CMA in the nervous system in particular, has just started to gain attention.

CMA has been also reported to protect neurons against stressors, since it is implicated in the degradation of the transcription factors myocyte-specific enhancer factor 2A (MEF2A) and 2D, (MEF2D) which are required for neuronal survival (Yang et al. 2009; Zhang et al. 2014). In non-neuronal cells it has been shown that CMA can regulate the growth of tubular kidney cells through degradation of the transcription factor Pax2 (Sooparb et al., 2004), the antigen presentation in dendritic cells (Zhou et al., 2005) and the control of NF-kB-mediated transcription through the degradation of IkB in Chinese hamster ovary cells during starvation (Cuervo et al., 1998).

Interestingly, environmental factors such as neurotoxins have been shown to have an impact on CMA activity. Marin et al. examined the expression levels of CMA markers in the substantia nigra of 6-hyroxydopamine (6-OHDA)-lesioned hemiparkinsonian rats. They found that the levels of LAMP2A and Hsp90 were increased in the substantia nigra ipsilateral to the 6-OHDA-evoked lesion, associated with a robust decrease in TH expression levels in the striatum (88%), providing *in vivo* evidence for a toxin-induced upregulation of CMA activity (Marin and Aguilar, 2011). Similarly, Gao et al. found that 6-OHDA-mediated oxidative stress induced MEF2D oxidation and increased LAMP2A levels, both in a dopaminergic cell line and in the mouse substantia nigra pars compacta, resulting in accelerated degradation of MEF2D (Gao et al., 2014). Reducing MEF2D or LAMP2A levels in the cell lines exacerbated 6-OHDA-induced death, whereas expression of an oxidation-resistant MEF2D mutant protected cells from 6-OHDA-induced death (Gao et al., 2014). Accumulation of the CMA substrates alpha-synuclein and MEF2D has been also observed upon exposure of SH-SY5Y neuroblastoma cells to the mitochondrial toxin rotenone (Sala et al., 2013). However, these changes in alpha-synuclein and MEF2D protein levels were due to changes in the regulation of their *de novo* synthesis rather than inhibition of their CMA-mediated degradation (Sala et al., 2013). Moreover, it was shown that hypoxic stress both in neuroblastoma cells and *in vivo* upon middle cerebral artery occlusion, increased LAMP2A protein levels and induced accumulation of LAMP2A-positive lysosomes in the perinuclear area, which is a hallmark of CMA activation (Dohi et al., 2012). This induction of CMA was neuroprotective, as blocking CMA using siRNA against LAMP2A accelerated cell death, whereas administration of mycophenolic acid, a potent CMA activator, rescued hypoxia-mediated cell death, suggesting that CMA is activated during hypoxia and contributes to the survival of cells under these conditions (Dohi et al., 2012).

Loss of CMA in the liver due to LAMP2A silencing caused hepatic glycogen depletion and hepatosteatosis; the liver phenotype was accompanied by reduced peripheral adiposity, increased energy expenditure, and altered glucose homeostasis (Schneider

et al., 2014). Comparative lysosomal proteomics revealed that key enzymes involved in carbohydrate and lipid metabolism are normally being degraded by CMA and loss of their regulated degradation contributed to the metabolic abnormalities observed in CMA-defective animals (Schneider et al., 2014). CMA decline, occurring with age, may be related with the metabolic dysregulation in aged organisms. This decline is a direct result of a decrease in the levels of the CMA receptor, LAMP2A, at the lysosomal membrane (Kiffin et al. 2007).

It seems that changes in the lipid composition of the lysosomal membrane with age are responsible for the loss of LAMP2A stability (Rodriguez-Navarro et al. 2012; Kiffin et al. 2007). Genetic manipulations restoring CMA function in aged mouse liver led to remarkable protection of aged livers from stressors and to an overall improvement in proteostasis and organ function (Zhang and Cuervo 2008). With regard to neuronal diseases, it would be of great importance to elucidate the physiological role of CMA in the brain and assess the consequences of the failure of this pathway in brain physiology and pathology. Preventing the systemic decline of CMA with age may prove an attractive strategy against organism functional loss and age-associated disorders.

### *A.7 CMA impairment and neurodegeneration*

Given the important role of CMA in maintaining cellular homeostasis, the potential role of CMA dysfunction in the pathogenesis of neurodegenerative diseases has started to gain ground. As mentioned above a common denominator in many neurodegenerative conditions is the aberrant accumulation of protein inclusions or aggregates in the cytosol of the affected neurons indicative of a failure of protein degradation systems. Both down-regulation and compensatory up-regulation of CMA activity have been reported in neurodegenerative conditions (Thompson et al. 2009, Alvarez-Erviti et al. 2010, Koga et al.2011, Xilouri et al.2016).

CMA contributes to the degradation of several proteins that have a propensity to aggregate and, as a result, CMA dysfunction leads to the accumulation of toxic protein aggregates. CMA can only degrade the soluble forms of these proteins. Once insoluble inclusions are formed, they are much more resistant to CMA-mediated degradation. These aggregates may often exert a “clogging or blockage effect” at the lysosomal membrane, thus blocking the degradation of other CMA substrates, leading to a vicious cycle of neurotoxicity (Cuervo et al. 2004, Martinez-Vicente M et al. 2008). Although it is not clear whether CMA dysfunction may contribute to the initial formation of insoluble inclusions, it is quite possible that the “blockage effect” may increase the concentration of misfolded protein concentrations, leading to the formation of inclusion bodies.

The first connection between CMA malfunctioning and a human disease was with PD (Cuervo et al. 2004). Since then, CMA failure has been linked to the pathogenesis of a growing number of neurodegenerative disorders such as AD, frontotemporal lobar degeneration and ALS. Disease-related proteins validated as CMA substrates include the PD-linked proteins α-synuclein, leucine-rich repeat serine/threonine-protein kinase 2 (LRRK2), UCH-L1, the AD and PD-linked Tau protein and huntingtin protein in Huntington's disease. However, it is possible that a larger number of proteins that are associated with neurodegeneration are CMA substrates, as many other proteins in these diseases contain KFERQ-like targeting motifs, or may acquire one upon translational modification (Lv et al. 2011; Thompson et al. 2009).

### *A.8 CMA and Parkinson's disease: Lessons from α-Synuclein*

Parkinson's disease (PD) is the second most common neurodegenerative disorder affecting approximately 1% of individuals older than 60 years. The primary neuropathological hallmark of PD is the loss of pigmented dopaminergic neurons in the *substantia nigra pars compacta* (SNpc), and their projections to the striatum. The loss of DA producing cells results in a deficit in striatal DA levels, leading to most of the clinical symptoms that characterize the disease. The presence of Lewy bodies (LB) and Lewy neurites (LN) in the remaining dopaminergic neurons is another common histopathological feature of the disease (Lewy et al. 1912; Spillantini 1997; Forno et al. 1996) These LB's and LN's contain proteinaceous intracellular inclusions rich in aggregated proteins, such as the neuronal protein α-synuclein, ubiquitin, neurofilaments and other proteins (Beach et al 2010; Gelpi et al. 2014).

α-Synuclein is abundantly expressed in the nervous system and accounts for approximately 1% of total soluble cytosolic protein (Iwai et al., 1995). It is generally found to localize to the presynaptic terminals in the central nervous system and is thought to be involved in the regulation of synaptic vesicle turnover and neurotransmitter release (Clayton and George 1998, 1999; Spencer et al. 2009). It is considered to be a natively unfolded protein, but it can be also found in several conformation states and aggregated morphologies. The propensity of α-synuclein to aggregate lies in the core of its neurotoxic potential (Martinez-Vicente et al. 2008). During the aggregation process, relatively soluble oligomeric α-synuclein species are formed, which then can self-assemble into fibrillar structures and become more and more insoluble (Conway et al., 1998). These intracellular entities or bodies containing aggregates of α-synuclein are called LBs in PD and DLB (Spillantini et al. 1997, 1998), glial cytoplasmic inclusions in MSA (Gai et al. 1998) and axonal spheroids in neuroaxonal dystrophies (Newell et al. 1999).

The first connection between CMA and PD has been established in the study of Cuervo et al. where monomeric and dimeric α-synuclein species were shown to be a substrate of CMA, bearing the VKKDQ motif (KFERQ-like) in its sequence. In the same study it was shown, that PD-linked mutant forms of α-synuclein (A30P and A53T) bound more tightly to LAMP2A at the level of the lysosomal membrane compared to the wild-type protein, but were not uptaken and degraded within lysosomes, thus becoming toxic by inhibiting the CMA-mediated degradation of other cytosolic substrate proteins (Cuervo et al., 2004). In agreement with these findings, lysosomal inhibition has been shown to cause an accumulation of α-synuclein, suggesting that the autophagy/lysosomal pathway is involved in the clearance of oligomeric and fibrillar species of the protein (Lee et al., 2004; Vogiatzi et al., 2008; Sacino et al., 2017). However, the mechanisms by which α-synuclein is degraded under normal and pathological conditions remain largely unknown.

Studies employing siRNAs against LAMP2A, CMA's rate-limiting step, as well as mutant forms of a-synuclein lacking the CMA recognition motif, verified that wild type α-synuclein is degraded via CMA in PC12 and SH-SY5Y cell lines and in primary neurons (Vogiatzi et al. 2008). In these cellular systems, CMA inhibition led to the formation of detergent insoluble or high molecular weight oligomeric α-synuclein conformations, providing strong evidence that CMA represents a major pathway for α-synuclein degradation, whereas CMA dysfunction contributes to generation of such aberrant species and likely to α-synuclein related pathology (Vogiatzi et al. 2008; Xilouri et al., 2009). Furthermore, the expression of A53T PD-linked mutant α-synuclein or DA-modified forms of the wild-type protein is able to cause CMA impairment and consequently to block the degradation of long-lived proteins by blocking their translocation to the lysosomes, providing an explanation for the vulnerability of dopaminergic neurons in synucleinopathies **(Fig. 4).** The inhibitory role of pathogenic α-synuclein forms in CMA was also reported in an earlier study showing that post-translational modifications of wild-type α-synuclein, such as oxidation and nitration of the protein, altered its binding and uptake into lysosomes, while phosphorylation and DA-modification of α-synuclein almost completely prevented its degradation through the CMA pathway (Martinez-Vicente et al. 2008). These results underscore the possibility that alpha-synuclein might exert its toxic effects through direct interference with the CMA pathway, even in cases with sporadic PD, where there are no mutations in α-synuclein. In addition, Mak et al. provided indirect evidence that CMA is a main mechanism for α-synuclein degradation *in vivo*, at least under conditions in which α synuclein levels are induced above a certain threshold (Mak et al. 2010). In this study, mice exposed to the mitochondrial toxin paraquat or α-synuclein transgenic mice up-regulated lysosomal LAMP2A and degraded α-synuclein more efficiently (Mak et al. 2010). We have previously shown that boosting CMA function both in cellular models and in the rat substantia nigra, mitigates α-

synuclein-related toxicity (Xilouri et al, 2013). This is accomplished by inhibiting the formation of both monomeric and aberrant α-synuclein species, such as phosphorylated α-synuclein (S129) and higher molecular weight species. In the rat viral model of α-synucleinopathy, the CMA-dependent decrease in α-synuclein levels restores DA levels in the striatum and increases the survival of DA neurons in the SNpc, further supporting the idea that induction of CMA activity may represent a fruitful strategy for the treatment of synucleinopathies.

CMA however is not the only route for WT α-synuclein degradation. Contrary to previous findings (Webb et al. 2003), inhibition of macroautophagy, but not of the proteasome, significantly enhanced wild type α-synuclein levels (Vogiatzi et al. 2008). Other studies suggest that macroautophagy also contributes to the degradation of α-synuclein aggregates, in large part because α-synuclein has been shown to interact with autophagic markers in cell models (Crews et al., 2010; Tanik et al. 2013). α-Synuclein aggregates are predominantly co-localized with LC3 and p62 in neurons, suggesting an accumulation at the autophagosome stage of autophagy (Tanik et al., 2013). Hence, macroautophagic degradation of α-synuclein may be dependent on its conformation and post-translational modifications, although it is still not completely understood which pathway is preferred by neurons for degrading oligomeric and fibrillar α-synuclein species. Dimeric, but not larger oligomeric species of α-synuclein can be degraded by CMA (Martinez-Vicente et al. 2008), whereas it is likely that higher order oligomers and possibly more fibrillar conformations may be degraded by macroautophagy.

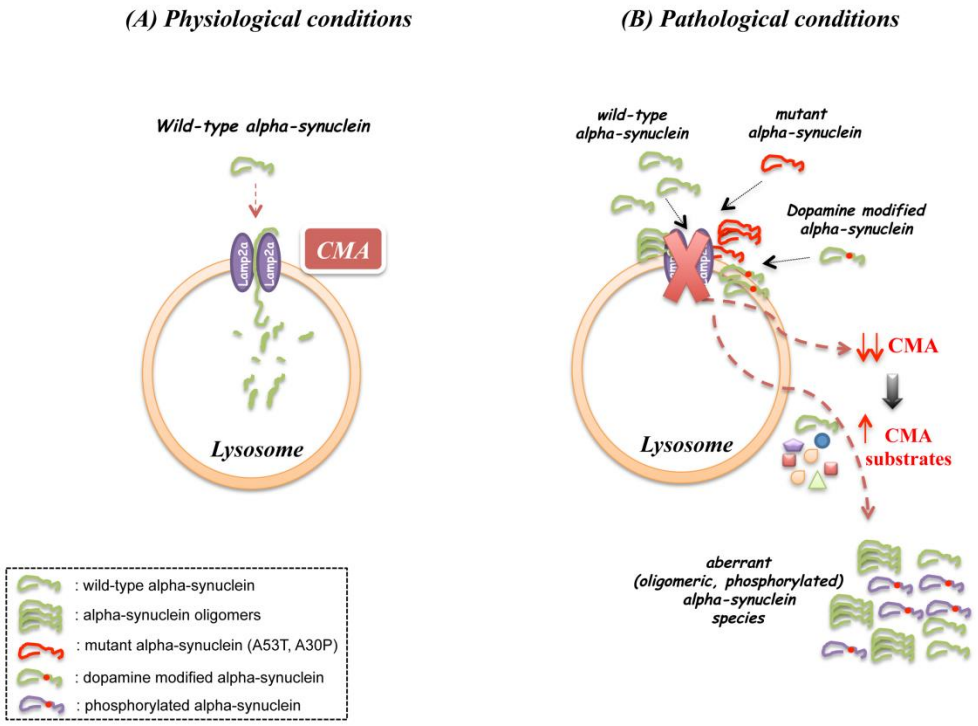


***Figure 4. Interplay between α-synuclein and CMA under physiological (A) and pathological (B) conditions.*** (A) Normally, WT α-synuclein is degraded by CMA, upon binding to the CMA-specific receptor, LAMP2A. (B) On the other hand, the PD-linked A53T and A30P mutants, as well as dopamine-modified α-synuclein, bind stronger to LAMP2A receptor and are not internalized, inhibiting both their own degradation and that of other CMA substrates. This CMA dysfunction results in accumulation of toxic α-synuclein species, which may lead to neuronal death.

A very interesting subject is the relationship between CMA and macroautophagy. Embryonic fibroblasts from Atg5 null mice showed higher constitutive CMA activity (Kaushik et al. 2008), leading to higher resistance to oxidative stress but more vulnerability to other stressors (Wang et al. 2008). A potential molecular link of CMA to macroautophagy could be provided by ubiquilin, which has been shown to be a substrate for both CMA and macroautophagy and can promote macroautophagy (Rothenberg et al. 2010). Another facet of CMA dysfunction that may be linked to neurodegeneration, involves effects on specific CMA substrates. In particular, overexpression of either WT or A53T α-synuclein led to CMA dysfunction, which in turn triggered mislocalization of the pro-survival transcription factor MEF2D to the cytosol, and loss of its activity. Interestingly, high cytosolic levels of MEF2D were detected in A53T transgenic mouse brain and in neuropathological material from PD nigra, suggesting that this abnormal effect evoked by CMA dysfunction may be important *in vivo* (Yang et al. 2009).

In order to elucidate whether such a relationship between CMA dysfunction and PD pathogenesis actually occurs in the human brain, recent studies have begun to investigate alterations of the main CMA components, HSC70 and LAMP2A, in human neuropathological material derived from PD patients. Chu et al. reported decreased HSC70 levels in PD nigra by immunohistochemistry, however other lysosomal components were also decreased, suggesting a more generalized lysosomal impairment, not specific to CMA (Chu et al. 2009). Alvarez-Erviti et al. using Western immunoblotting detected significant decreases in both HSC70 and LAMP2A in nigra and amygdala of PD brains compared to controls, whereas LAMP1 levels were unaltered (Alvarez-Erviti et al. 2010). Isolation of lysosomal membranes from the amygdala confirmed that the decrease in PD brains also applied to lysosome-associated LAMP2A, suggesting that there may be a specific widespread CMA impairment in PD brains, beyond areas with the confounding factor of neuronal cell loss and gliosis. No alterations in these CMA components were observed in AD brains. In a more recent study, PD-related correlations between β-glucocerebrosidase, CMA and alpha-synuclein in two brain regions, one with increased alpha-synuclein levels in PD (anterior cingulate cortex) and one without (occipital cortex), were assessed (Murphy et al. 2014). This study showed that the selective loss of lysosomal glucocerebrosidase early in sporadic PD was directly related to impaired CMA activity (but not macroautophagic), which was correlated with reduced LAMP2A and increased alpha-synuclein levels and decreased ceramide (Murphy et al. 2014). The same group examined expression levels (mRNA, protein) of all three LAMP2 isoforms in the aforementioned brain regions (anterior cingulate and occipital cortex), in correlation to alpha-synuclein pathology (Murphy et al. 2015). They found that in the early stages of PD, mRNA expression of all LAMP2 isoforms and protein levels of LAMP2B and LAMP2C were not different from controls. On the contrary, LAMP2A protein levels were found selectively decreased, directly correlated with increased levels of a-synuclein and decreased levels of HSC70 in the same PD samples, as well as with accumulation of cytosolic CMA substrate proteins, MEF2D and IkBα (Murphy et al., 2015). This study suggests that CMA dysregulation may precede substantial alpha-synuclein accumulation in PD and supports further the idea of targeting the CMA pathway for the treatment of PD and other synucleinopathies. Another report showed that deregulation of microRNAs in PD brains may underlie the down-regulation of some CMA components in the affected neurons (Alvarez-Erviti et al. 2013). In addition, a sequence variation in the promoter region of LAMP2 identified in a PD patient (Pang et al. 2012) opens up the possibility that alterations in CMA components may underlie some forms of PD.

Beyond the CNS, three studies have identified alterations in the levels of the key CMA markers, LAMP2A and HSC70, in the periphery of sporadic PD patients, utilizing peripheral blood mononuclear cells (PBMCs). More specifically, Wu et al. found that

LAMP2 gene expression and protein levels in PBMCs of sporadic PD patients were significantly decreased compared to controls, while at the same time LC3 gene expression and LC3-II protein levels were significantly increased (Wu et al. 2011). These results suggested a decreased CMA activity with a compensatory aberrant accumulation of autophagosomes in peripheral tissues of PD patients. Recently, another study showed reduced protein and mRNA expression of HSC70 in PBMCs of sporadic PD patients compared to age-matched controls, both under basal conditions and upon autophagy induction (Sala et al. 2014). No difference was detected in LAMP2A and MEF2D expression between patients and controls. Our lab, in general agreement with these results, has also found decreased HSC70 mRNA and protein levels in sporadic PD (Papagiannakis et al., 2015). Such studies suggest a systemic LAMP2A (Wu et al. 2011) or HSC70 (Sala et al. 2014, Papagiannakis et al., 2015) reduction in PD patients, possibly related to a more generalized CMA dysfunction in this disease.

### *A.9 Crosstalk between Macroautophagy and CMA*

That said, it becomes evident that proper protein quality control is intrinsically challenging in neurons because of their unique architecture, in which specific compartments such as synapses are distant and functionally distinct from the soma, with their own pool of proteins (Wilhelm et al. 2014). Moreover, a delicate balance between the various degradation pathways is essential in maintaining cellular homeostasis. Several studies have demonstrated a close crosstalk between CMA and macroautophagy in many cellular systems, where blockage of one of these pathways results in upregulation of the other (Massey et al. 2006, Kaushik S et al. 2008). Massey et al. reported for the first time that blockage of CMA in cultured cells results in "productive", activation of macroautophagy and to degradation of substrate proteins within lysosomes. More specifically, it has been demonstrated that in the early stage after CMA blockage by RNA interference against the lysosomal membrane receptor, LAMP-2A, its macroautophagic activity decreases because of an increase in mTOR activity. However, as CMA blockage persists, the increased intracellular levels of Beclin 1, along with the reduced phosphorylation of mTOR, can work together to induce constitutive activation of the macroautophagy (Massey et al 2008). However, the molecular mechanisms underlying the cross-talk among these different pathways have not been yet fully elucidated. Recentrly, Wang et al. reported that phosphorylation of ULK1, a central kinase of the ULK1 complex involved in autophagy initiation, affects autolysosome formation and links CMA to macroautophagy. More specifically, they demonstrated that phosphorylation of ULK1 through PKCa enhances its interaction with HSC70 and increases its degradation through CMA maintaining the balance of macroautophagy activation (Wang et al. 2018).

Despite the fact that autophagic pathways are not redundant, they can compensate for each other at least under basal cellular conditions. Macroautophagy serves as a backup mechanism to remove malfunctioned proteins (i.e., aberrant α-synuclein in the case of PD) from the cytoplasm when CMA is compromised, and vice versa. This compensation is only partial, as, for example, organelles normally degraded by macroautophagy cannot undergo degradation via CMA. Although replacement of one type of autophagy could be a cellular protective response, cells with compromised CMA become vulnerable to a myriad of cellular stressors due to the compensatory activation of macroautophagy observed in these cells (Massey 2006).

## B. Aim of the Study

Increasing evidence demonstrates that malfunction of CMA plays a key role in the pathogenesis of severe human disorders including PD and other neurodegenerative disorders. In order to study the consequences of CMA impairment in the rodent nigrostriatal system we have recently generated a novel rat model, in which viral-mediated downregulation of LAMP2A, CMA's rate-limiting step, within the SNpc leads to progressive loss of dopaminergic neurons, loss of striatal dopamine, and accumulation of α-synuclein, thus mimicking key aspects of PD (Xilouri et al. 2016).

Aim of the current study was to determine the contribution of macroautophagy to the axonal degeneration that occurs early in this model well before cell soma degeneration becomes evident (8 weeks post-injection), a phenomenon called "retrograde axonopathy". In this system, we have observed a marked accumulation of autophagic vacuoles and biochemical indices suggestive of enhanced productive macroautophagy in the nigral cell bodies of dopaminergic neurons at 8 weeks post-injection (Xilouri et al., 2016). We hypothesize that this likely excess compensatory activation may be linked to the phenomena of dopaminergic axonal degeneration. As a first step in the investigation of this hypothesis, it is crucial to investigate in further detail the relative timing of the induction of macroautophagy and its relationship to terminal degeneration.

For this purpose, injections of rAAV vectors bearing a shRNA sequence against the cytosolic tail of LAMP2A or a scrambled sequence that have been previously described (Xilouri et al, 2016), were performed unilaterally in the SNpc of 8 week old young female HAN-Wistar rats. Biochemical and immunohistochemical analyses were performed in the brain tissues from these rats at 2 and 3 weeks post injection.

We have initially examined whether such induction of macroautophagy may occur in this model at the level of the striatal dopaminergic terminals, as well as in the nigral cell bodies, at these early time points, using electron and confocal microscopy. We have also assessed the integrity of the nigrostriatal projections with densitometry of the striatal dopaminergic neuronal terminals, as well as the relative astro- and micro-gliosis in the nigrostriatal axis, as possible activation of these glial cells may contribute to the neurodegenerative effect observed at the later time points.

# C. Materials and Methods

### *C.1 Animals*

Eight-weeks-old young female HAN-Wistar rats (180-200 g) were housed (3-4 animals/cage) with free access to food and water under 12-h light/dark cycle. All experimental procedures performed were approved by the Ethical Committee for Use of Laboratory Animals in the Biomedical Research Foundation of Athens.

### *C.2 Surgical Procedures*

All surgical procedures were performed under isoflurane anesthesia. After placing the animal into a stereotaxic frame, 2 µL of rAAV solution (with final titer of 7E13 gc/mL) was injected unilaterally into the right SN using the following coordinates: −5.0 mm anteroposterior, −2.0 mm mediolateral from the bregma, and −7.2 mm dorsoventral from the dura, according to the rat stereotaxic atlas (Paxinos and Watson 1998). The tooth bar was adjusted to −2.3 mm. Injection was performed using a pulled glass capillary (diameter of approximately 60–80 µm) attached to a Hamilton syringe with a 22s gauge needle. After delivery of the viral vector using an injection rate of 0.1 µL/15 sec the capillary was held in place for 5 min, retracted 0.1 µm, and, after 1 min, was slowly withdrawn from the brain.

### *C.3 Perfusion, fixation and sectioning of rat brains*

Rats were anesthetized with isoflurane and perfused intracardially with phosphate-buffered saline (PBS; Thermo Fisher Scientific, 70011036), followed by ice-cold fixative 4% paraformaldehyde (PFA, Sigma Aldrich, P6148). Following perfusion, rats were decapitated and the brains were removed. The brains were post-fixed for 24 h in the same preparation of paraformaldehyde and then transferred to 15% sucrose overnight, before being incubated in 30% sucrose until freezing. The brains were frozen in 2-methylbutane (Isopentane) at -45$^0$C for 30-50 min and stored at -80$^o$C. Fourty µm sections were prepared using a cryostat at -25°C. Free floating sections encompassing the striatum and the SNpc were collected into a 12 well plate in anti-freeze solution (for 2.133L: 3.349g $NaH_2PO4$, 11.627g $Na_2HPO4$, 853.3 ml H2O, 640 ml ethylene glycol, 640 ml glycerol), and were kept at -20°C until staining.

### *C.4 Immunofluorescence*

For immunofluorescence assay, tissue sections were washed 3 times with PBS (3x10 min) and incubated with 0.1M sodium citrate solution (pH 8.5-9.0) 30 minutes at 80$^{o}$C in a water-bath, followed by 20 min incubation on ice. After 3 washes with PBS, tissues were incubated for 1 hour in blocking solution (5% NGS, 0.1% Triton in PBS) at room temperature (RT). After blocking, sections were incubated with the primary antibodies (2% NGS, 0.1% Triton in PBS) **(Table 1)** overnight at 4°C. After three washing steps of 10 min each with PBS, sections were incubated with the secondary antibodies for one hour, in RT. The fluorescent secondary antibodies used were Biotium CF488A (1:2000; 20010 ms, 20012 rb, 20020 ck), Biotium CF555 (1:2000; 20030 ms, 20033 rb), and Jackson Immunoresearch Affinipure Cy5 (1:400, 115-175-146). For the fluorescent staining of the nuclei, the 4',6-diamidino-2-phenylindole (DAPI) stain was additionally used (1:2000). Finally, after 3 washes with PBS the sections were rinsed with PBS and mounted on poly-D-lysine coated glass slides.

### *C.5 Automated image analysis*

Confocal z-stacks of 1024 × 1024 pixels were collected throughout the whole optical thickness of the mounted sections using a z-step of 0.9 microns, imaging through a Leica TCS SP5 confocal microscope (Wetzlar, Germany). Immunolabeled samples were imaged using an oil-immersion Leica HCX APO 63×1.20 objective or HCX APO 40×1.20 objective. Totally, 12-18 stacks were collected per animal, with an average 8-15 GFP$^{+}$ cell profiles visible in each field of view. Quantifications were done with the Imaris software suite (v7.7.2, Bitplane AG), using a static set of parameters to isolate GFP$^{+}$ cell profiles, and then masking the channel containing the LAMP2A, the LC3 and the SQSTM1/p62 signal using said profiles. The masking of the GFP$^{+}$ signal was based on intensity and sphericity and the quantification of immunofluorescent puncta in other channels filtered by the GFP$^{+}$ mask was done using the automated spot counter plug-in. For GFAP, IBA1, DAT and Bassoon quantifications, total fluorescence was measured and normalized to the average background signal of the whole image. Values from all stacks were averaged to produce a single value per animal, and data are expressed as fold change of the average in the scrambled control group.

### *C.6 DAB immunostaining*

To evaluate the integrity of the dopaminergic nigrostriatal terminals, coronal striatal sections were immunostained for Tyrosine Hydroxylase (TH) using the 3,3'-diaminobenzidine (DAB). The selected sections were incubated for 10 min in a 10% MeOH/3% $H_2O_2$ solution (in PBS), followed by blocking of the non-specific sites with 5% NGS in PBS. The primary antibody against mouse TH in a dilution of 1:5000 for striatal sections was solubilized in NGS 2% (in PBS) and the incubation was done for 48 h. The secondary biotinylated rabbit antibody was subsequently used (1:3000; 60 min in NGS 2% in PBS), followed by incubation with the ABC solution (Elite ABC kit, Vector) and staining with DAB (DAKO), according to manufacturer's instructions. The sections were afterwards mounted and dehydrated.

### *C.7 Densitometry*

Striatal dopaminergic neuronal terminal density was measured using every sixth coronal section of the animal's striatal tissue, covering the whole rostro-caudal axis of the striatum. The regions of interest were outlined and the density of the TH-positive terminals, controlling for the background cortex, was measured in the injected and the non-injected side in every section using Gel analyzer v1.0 software. The data are presented as means from all animals and expressed as the ratio to the contralateral side.

### *C.8 Electron microscopy*

*Tissue preparation*: Rat brain tissues were prepared according to Moss and Bolam 2008). Briefly, animals were perfused intracardially through the ascending aorta with 50 ml PBS under isoflurane anesthesia, followed by 200 ml of fixative (0.1 M phosphate buffer, pH 7.4, 3% paraformaldehyde, 0.1% glutaraldehyde [Sigma-Aldrich, G5882]) for 25 min. Free fixative was removed by post-perfusion with PBS and brains were removed and sectioned through the coronal plane at the level of SNpc at 65-mm increments, using a vibrating blade microtome (VT1000S, Leica, Wetzlar, Germany).

*Immunohistochemistry:* Pre-embedding immunohistochemical procedures (immunogold-silver and immunoperoxidase labeling) were performed on free-floating sections as described (Miner et al. 2006) with some modifications. Briefly, 65-µm-thick sections were blocked, incubated overnight with the GFP antibody (1:50), followed by incubation with nanogold anti-mouse IgG (1:50; Nanoprobes, 2001) and HQ Silver enhancement (Nanoprobes, 2012). The sections were finally post-fixed with osmium tetroxide, dehydrated in an ascending ethanol series, flat-embedded in epoxy resin

[mixture of Glycid Ether 100 (Serva, 21045.02), 2-Dodecenylsuccinic-acid anhydrade (Serva, 20755.02), 2,4,6-Tris (dimethyl-aminomethyl) phenol (Serva, 36975.01), Remlan M-1 (Serva, 13825.02) and Di-n-butyl phthalate, 99% (Alfa Aesar, A13257)] using ACLAR Film (EMS, 50425) and the specimens were allowed to polymerize at 60°C for 24 h. All sections were examined under the light microscope and the selected small areas from the SNpc or the striatum right and left, were cut, re-embedded on the top of resin blocks and polymerized again at 60°C for 24 h. Ultrathin sections (65-nm thick) cut in a Leica EM UC7 Ultramicrotome (Leica Microsystems, Vienna, Austria) were lead-stained and examined under a Philips EM 420 electron microscope (Philips Electron Optics, Eindhoven, The Netherlands).

### *C.9 Preparation of Synaptosomes*

After decapitation, striatum was dissected out on ice and preparation of synaptosomes was performed as described by Biesmann et al. (2013). The tissues from the injected and uninjected hemispheres were homogenized in 1 ml of ice-cold homogenization buffer (0.32 M Sucrose, 4 mM HEPES pH 7.4) containing 1X protease inhibitors cocktail plus 1X PhosSTOP Phosphatase Inhibitor Cocktail (for phospho proteins) (Roche) using a 5-ml glass-Teflon homogenizer with 12 gentle strokes. The homogenizer was then rinsed with additional 1 ml of homogenization buffer and then centrifuged at 1000 g for 10 min at 4°C in an SS-34 rotor (Sorvall). The supernatant (S1) was removed from the pellet (P1) and centrifuged at 12,500 g for 15 min at 4°C in an SS-34 rotor. The supernatant (S2) was removed completely and the synaptosome-enriched pellet (P2) was resuspended in 0,5 ml of homogenization buffer. The re-suspended pellet (P2 fraction) was then layered over a discontinuous sucrose gradient (0.85–1.0–1.2 M) and centrifuged at 50,000 g for 70 min at 4°C in an SW-41Ti rotor (Beckman). The synaptosome-enriched fraction was recovered at the interface of 0.8 and 1.2 M sucrose using a glass Pasteur pipette.

### *C.10 Western blotting*

For the biochemical analysis of the synaptosomal preparations, the brains were harvested, dissected on ice to obtain the region of interest, and frozen immediately. All animals were processed in a similar manner. Tissue was stored at −80°C until further use. After synaptosomes preparation, as described above, the synaptosome-enriched fraction certifuged at 50.000g for 20 min 4°C. The supernatant (S3) was collected and the synaptosome-enriched pellet (P3) was resuspended in PBS containing 1X protease inhibitors cocktail plus 1X PhosSTOP Phosphatase Inhibitor Cocktail (for phospho proteins) (Roche).

Bradford method was used to measure the concentration of proteins in samples and the proteins were electrophoresed on a 12% polyacrylamide gel. Proteins were transferred to a nitrocellulose membrane (400 mA for 2 hours) before blocking in 5% milk for 1hour. Mebranes were then incubated overnight at 4°C in the primary antibodies, shown in Table 1. Then, membranes were washed three times (3x10min) with TBST (100 mM Na2HPO4, 100mM NaH2PO4, 0.5N NaCl, 0.1% Tween-20), and incubated with secondary horseradish peroxidase-conjugated-HRP antibodies (1:10000) for 1 hour at RT. Membranes were washed three times (3x10min) with TPBS and then developed with chemiluminescent solution.

*To re-probe membranes with a different primary antibody,* membranes were incubated in Stripping buffer (0.2M Glycine, 0.5M NaCl, pH 2.6) for about 30 mins with constant agitation at room temperature, followed by 3x washes with TBST and re-blocking with 5% BSA/TBST blocking buffer for 30mins, prior to incubation with another primary antibody.

***Table 1. List of antibodies used for immunofluorescence (IF) and Western Blot (WB) studies.***

| **Primary antibodies for Immunofluorescence (IF) & Western Blot (WB)** | | | | |
|---|---|---|---|---|
| **Antibody** | **Host** | **Source** | **Cat. No** | **Working dilution** |
| AIF1/IBA1 | rabbit | WAKO | 19741 | 1:1000 (IF) |
| Bassoon | mouse | Enzo | 4071513 | 1:500 (IF) |
| Dat | rat | Millipore | MAB369 | 1:1000 (IF) |
| Glial Fibrillary acidic protein (GFAP) | rabbit | Dako | Z0334 | 1:750 (IF) |
| Green Fluorescent Protein (GFP) | chicken | Abcam | ab13970 | 1:2000 (IF) |
| LAMP2A | rabbit | Zymed Laboratories | 51-2200 | 1:800 (IF) |
| LC3 | rabbit | MBL | PM036 | 1:1000 (IF) |
| SQSTM1/p62 | rabbit | MBL | PMO45 | 1:1000 (IF) |
| Synaptophysin | mouse | SySy | 101011 | 1:1000 (WB) |
| TUBG/tubulin gamma | mouse | Sigma-Aldrich | T5326 | 1:2000 (WB) |
| Tyrosine Hydroxylase (TH) | mouse | Millipore | MAB318 | 1:2000 (IF) |
| ULK-1 | rabbit | Cell Signaling | 8054S | 1:1000 (IF) |

# D. RESULTS

### *D.1 Efficient transduction of the rat nigrostriatal pathway with rAAVs*

In order to inhibit CMA, dopaminergic neurons were stereotactically injected with rAAVs (7E14 gc/ml) expressing shRNAs targeting endogenous rat LAMP2A (L2) or scrambled control shRNA (scr) and the animals were sacrificed at 2 and 3 weeks post-injection. These viruses contained GFP under the control of the neuronal promoter synapsin (SYN1), thus enabling the visualization of the transduced neurons with the respective shRNAs. LAMP2A is the rate-limiting step of CMA and thus a decrease in its levels results in reduced CMA activity. The efficient transduction of the majority of tyrosine hydroxylase (TH)-positive nigral dopaminergic neurons (**Fig.1A, upper row)**, as well as their projections to the striatum (**Fig. 1B, bottom row)**, in the injected (ipsilateral) hemisphere was demonstrated by immunohistochemistry, where a co-localization of TH with the GFP reporter was observed throughout the whole nigrostriatal axis, assessed at 3 weeks post-transduction.

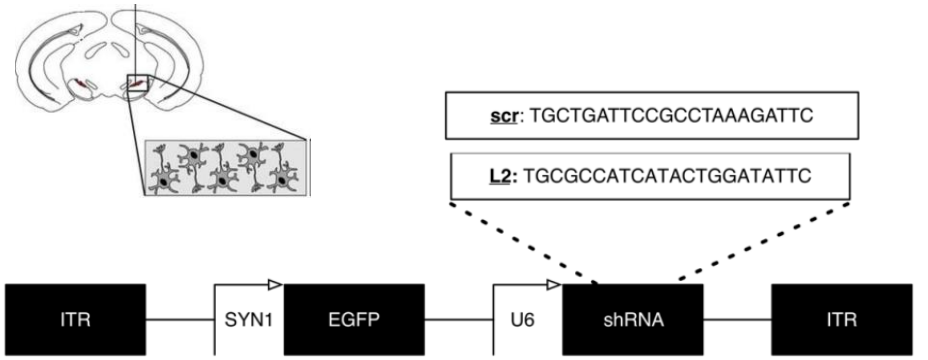


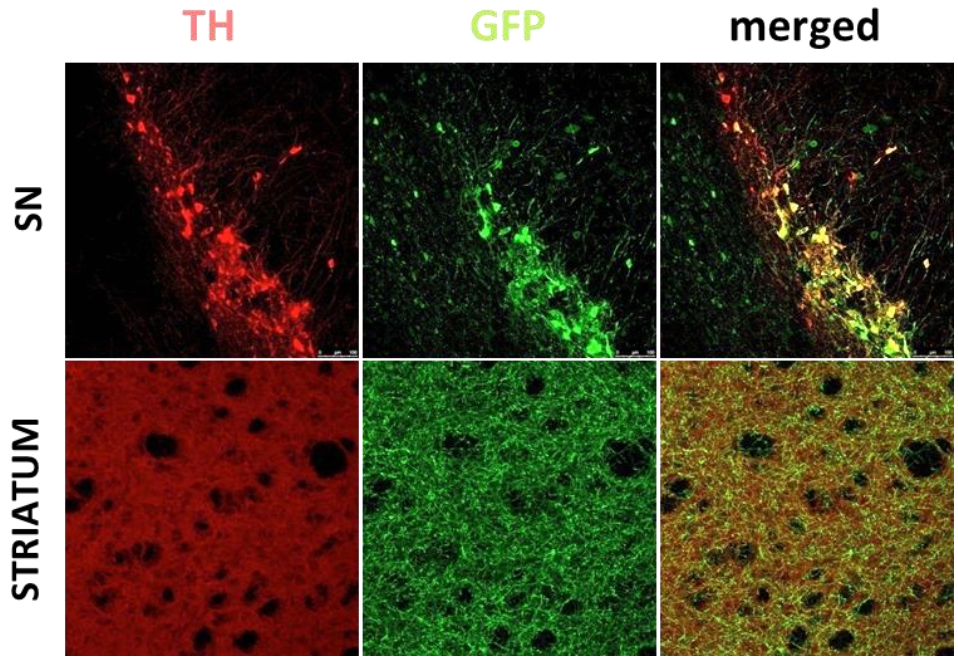

***Fig. 1: Generation and efficient delivery of rAAV-vectors targeting endogenous LAMP2A in the rat nigrostiatal pathway. (A)*** *Schematic representation of rAAV-vector design, with the LAMP2A-specific targeting sequence (denoted L2) and the scrambled control sequence (scr), listed in full.* ***(B)*** *Efficient delivery of rAAV-vectors targeting endogenous LAMP2A in the rat nigrostiatal pathway. Representative immunofluorescence images with tyrosine hydroxylase (TH) and GFP antibodies showing the expression of the GFP-tagged rAAV-scr shRNA vector in the $TH^+$ neurons of the substantia nigra (SN) (upper row) and their $TH^+$ striatal efferents (bottom row), at 3 weeks post-injection. Scale bar: 100 μm for SN and 50 μm for striatum.*

### *D.2 Downregulation of LAMP2A in transduced dopaminergic neurons*

The efficient downregulation of the LAMP2A receptor within transduced dopaminergic neurons was confirmed with confocal microscopy. Double immunostained midbrain sections with antibodies against LAMP2A and GFP **(Fig.2)** verified the efficient downregulation of LAMP2A in $GFP^+$ dopaminergic neurons, in the L2-shRNA AAV ipsilateral midbrain.

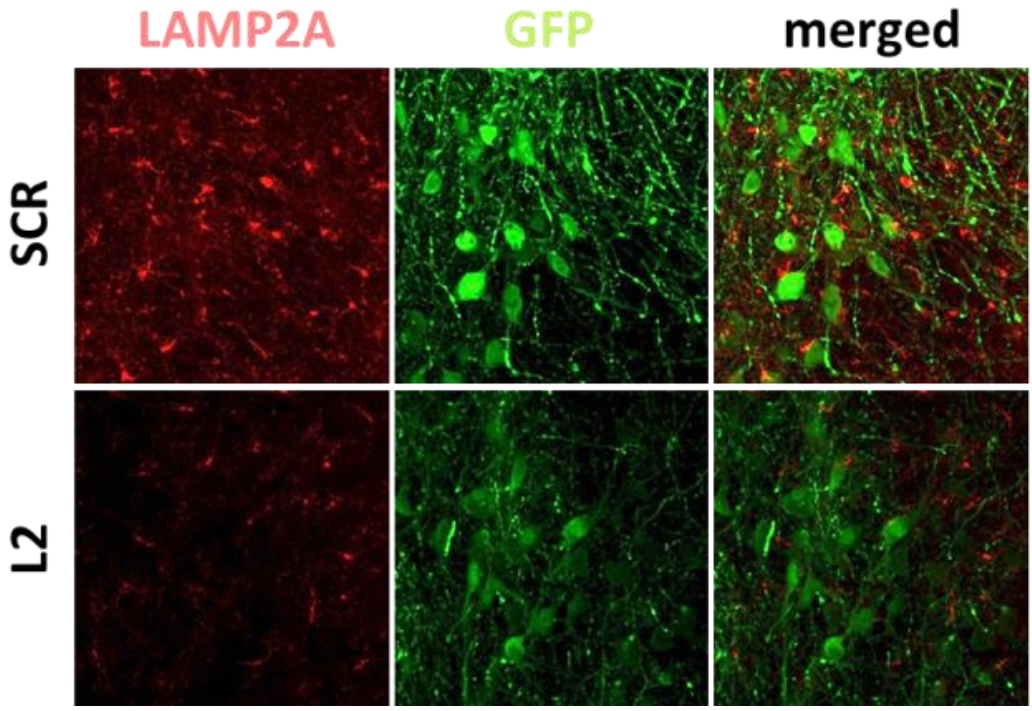


***Fig. 2: rAAVs expressing shRNAs against endogenous rat LAMP2A (L2) efficiently decrease LAMP2A protein levels in transduced $GFP^+$ nigral neurons.*** *Representative immunofluorescence images depicting the expression of LAMP2A in nigral neurons transduced with the GFP-tagged rAAV-shRNAs, at 3 weeks post-injection. Same results were obtained at 2 weeks post injection. Scale bar: 50 μm.*

### *D.3 CMA impairment is accompanied by increased LC3 levels and decreased SQSTM1/p62 levels within transduced degenerating nigral neurons*

It has been previously shown that selective blockade of CMA in cell cultures results in compensatory upregulation of macroautophagy that may be either beneficial or deleterious, depending on the system examined (Massey et al. 2006; Vogiatzi et al., 2008; Xilouri et al. 2009). In our model in particular, CMA impairment in the rat dopaminergic system leads to progressive degeneration of transduced nigral neurons, which is accompanied by increased abundance of autophagic vacuoles (AVs) and possibly increased autophagic flux, at 8 weeks post injection (Xilouri et al, 2016). In order to clarify the relationship of macroautophagy to the observed degeneration, we have examined here the induction of macroautophagy in the nigrostriatal pathway of LAMP2A-deficient rats at a time point prior to overt nigral cell loss.

Towards this direction, we assessed the levels of the autophagy marker protein LC3 (MAP1LC3B) within $GFP^+$ neurons in the ipsilateral midbrain of rats injected with the LAMP2A-shRNA-AAV and the scr-shRNA-AAV at successive time points of 2 and 3 weeks post injection. Conversion of LC3-I to LC3-II by the addition of phosphatidylethanolamine is essential for the formation of autophagosomes and is considered a marker of autophagosome formation and accumulation (Mizushima et al. 2010). In order to evaluate the levels of LC3, we employed unbiased automated single cell analysis using the Imaris software suite (v7.7.2, Bitplane AG), using a static set of parameters to isolate $GFP^+$ cell profiles, and then masking the channel containing the LC3 positive (red) signal using said profiles. The masking of the $GFP^+$ signal was based on fluorescent intensity **(Fig. 3).** The automated image analysis revealed increased LC3 levels for L2 (1,67±0,19) rAAV-injected animals compared to the scr-injected ones (1,00±0,09), at the 3-week time point, thus indicating that accumulation of autophagosomes represents an early event in our model. No statistically significant differences were observed at 2 weeks post injection between L2 (1,04±0.21) and scr (1,00±0.04) injected rats.

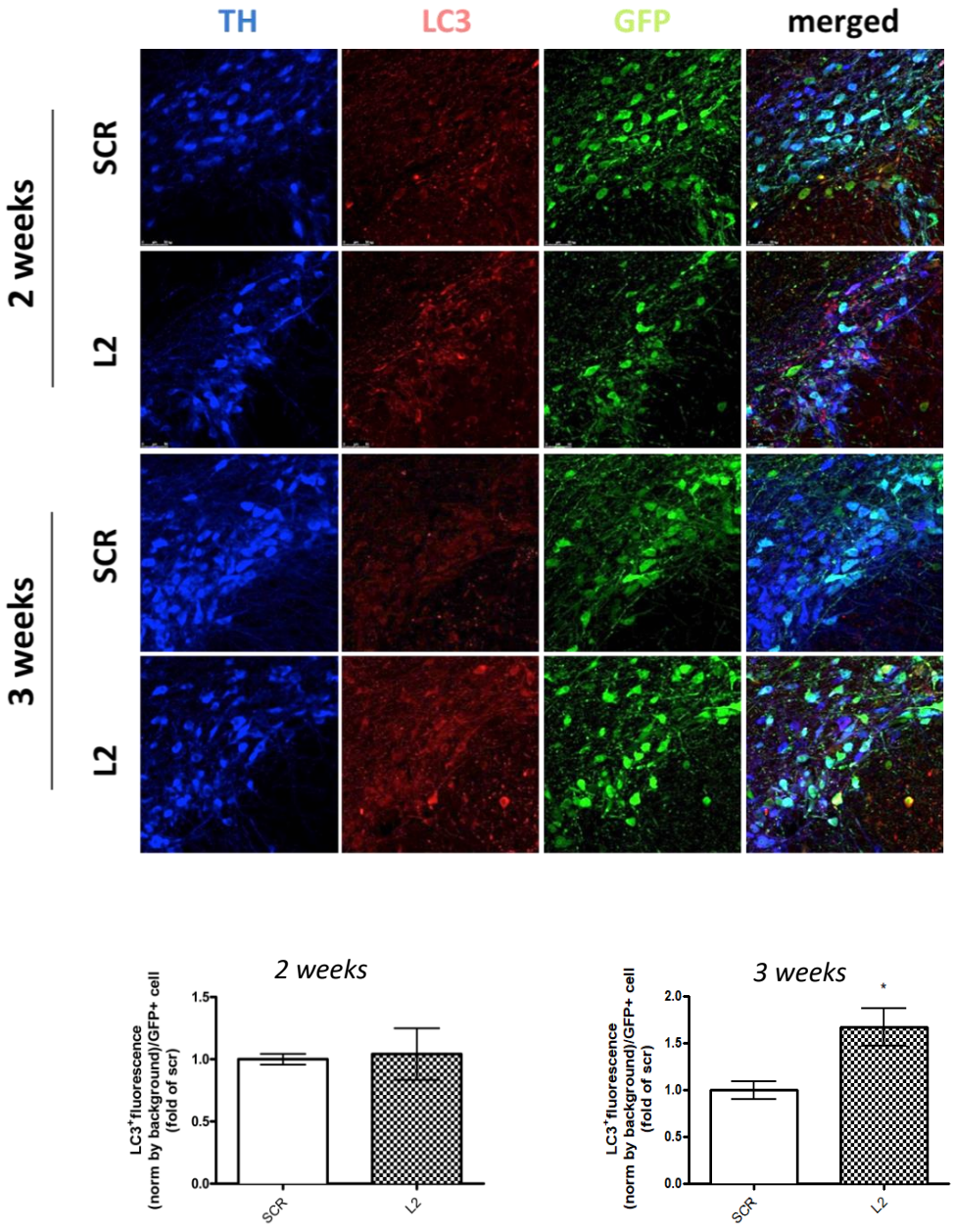


***Fig. 3: LAMP2A down-regulation is accompanied by increased LC3 levels within transduced nigral neurons, at 3 weeks post-injection.*** *Representative immunofluorescence images depicting LC3 levels within GFP$^+$ LAMP2A deficient nigral neurons at 2 and 3 weeks post-injection are shown in the upper panels. Scale bar: 50 µm. Quantifications of LC3$^+$ fluorescence/GFP$^+$ cell are shown in the bottom panels (*, $p < 0.05$; n =4 animals/group, t-test).*

Given the fact that increased LC3 levels are not always indicative of enhanced autophagic flux and may represent increased autophagosome formation or decreased degradation, we measured the levels of the selective autophagy receptor protein SQSTM1/p62. Based on the notion that SQSTM1/p62 is degraded via autophagy, monitoring degradation of SQSTM1/p62 is used to measure autophagic flux. To this end, midbrain sections were immunostained with antibodies against TH (blue), GFP (green) and SQSTM1/p62 (red) **(Fig. 4).** Quantification of total SQSTM1$^{+}$ fluorescence in GFP$^{+}$ neurons showed no difference in L2 AAV-injected rats (0,8 ± 0,77), compared with the scr AAV-injected control ones (1,00± 0,09), at 2 weeks post injection **(Fig. 4, upper panel).** However, at 3 weeks post injection, a statistically significant decrease of SQSTM1$^{+}$ fluorescence in GFP$^{+}$ neurons was detected in LAMP2A-deficient rats (0,53 ± 0,06), compared to the control scr-injected ones (1,00 ± 0,15), thus suggesting an accelerated clearance of SQSTM1/p62 through the macroautophagic pathway **(Fig. 4, bottom panel).**

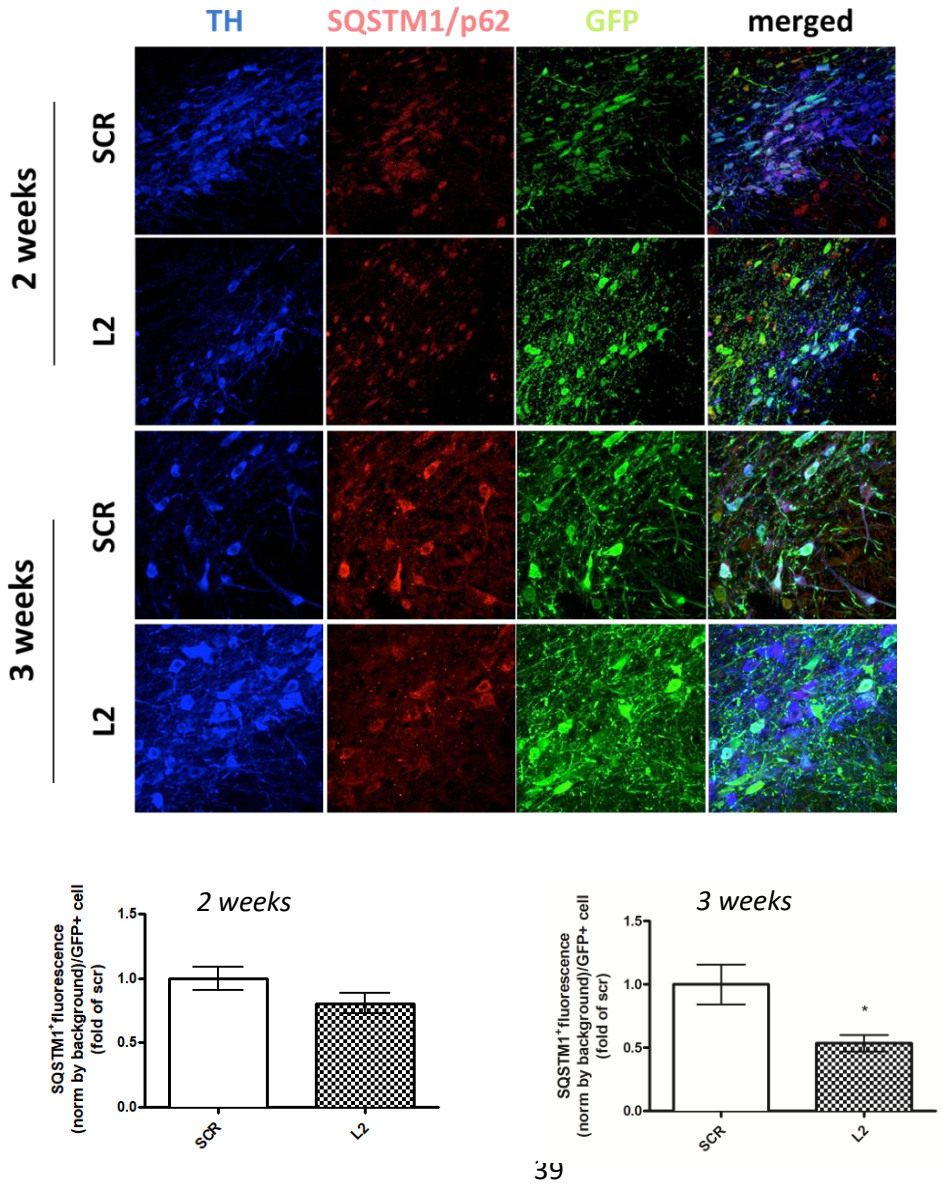

***Fig. 4: LAMP2A down-regulation is accompanied by decreased SQSTM1/p62 levels within transduced nigral neurons, at 3 weeks post-injection.*** *Representative immunofluorescence images depicting SQSTM1/p62 levels within GFP$^+$ LAMP2A deficient nigral neurons at 2 and 3 weeks post-injection are shown in the upper panels. Scale bar: 50 μm. Quantifications of SQSTM1/p62 fluorescence/GFP$^+$ cell are shown in the bottom panels (*,p=0,029; n =4 animals/group, t-test).*

### *D.4 CMA deficiency results in accumulation of AVs within GFP$^+$ transduced degenerating nigral neurons, at 3 weeks post injection*

To assess further the contribution of macroautophagy in our model at the ultra-structural level, we performed immunoelectron Microscopy (EM) analysis in the substantia nigra (SN) of scr and L2-injected rats, at 2 and 3 weeks post-injection **(Fig. 5).** Immunogold labeling for GFP, which was selectively expressed only in the TH-positive transduced neurons, was used to visualize them. The detection of AVs at the ultra-structural level was based on the established morphological characteristics: initial AVs contain intact cytoplasmic materials enclosed in a double-membrane structure, whereas late-stage degradative AVs upon fusion with late endocytic organelles, have only one limiting membrane and contain cytoplasmic material and/or organelles at different stages of degradation (Klionsky et al., 2012).

In scr-injected rats, the cytoplasm and the processes of GFP$^+$ nigral neurons had typical morphological features **(Fig. 5A,D).** In contrast, ultrastructural analysis of the LAMP2A-deficient nigral neurons at 2 and 3-weeks post-injection revealed the presence of numerous AVs with storage material in GFP$^+$ transduced degenerating neurons, mostly evident at 3 weeks post-injection **(Fig. 5C).** AVs were rarely seen in the processes of LAMP2A-deficient rats at 2 weeks post injection **(Fig. 5B)**, whereas the perikaryon of LAMP2A-deficient rats was characterized by the presence of AVs only at 3 weeks post injection (**Fig. 5F**)

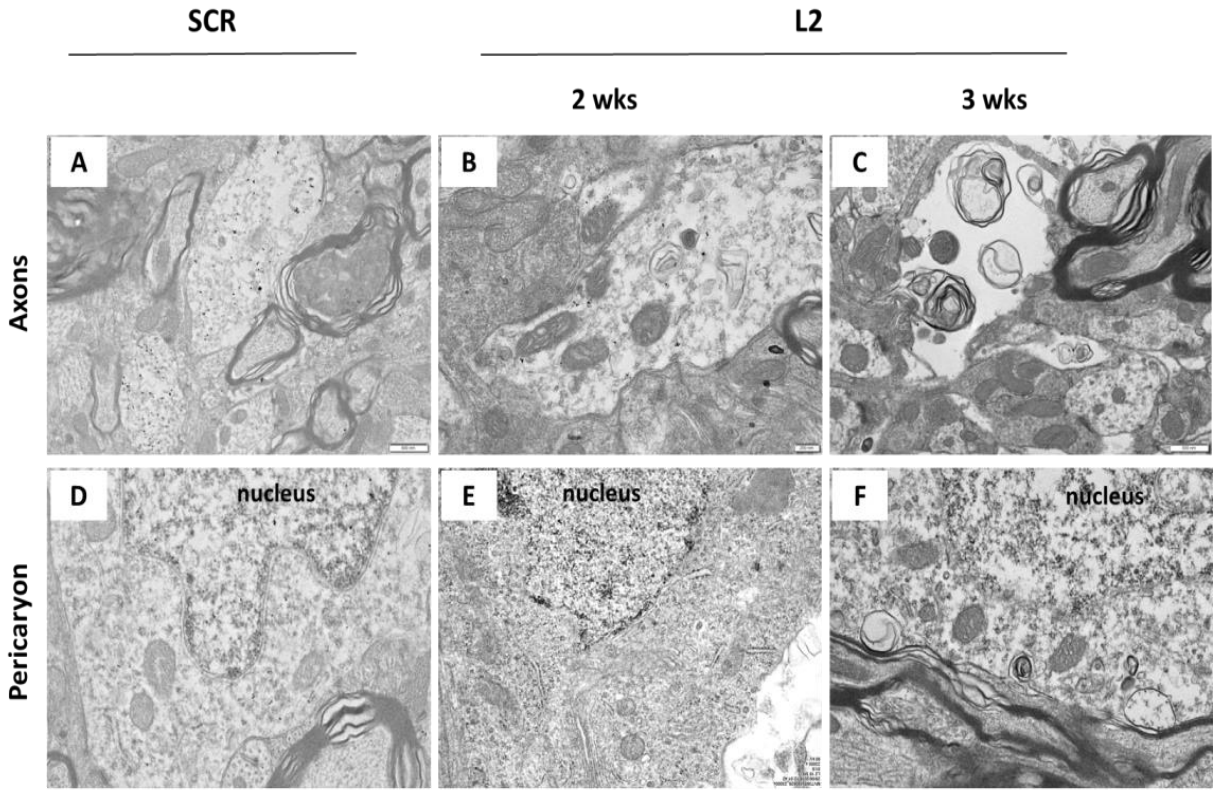


***Fig.5: Representative electron micrographs with immunogold labeling for GFP of the ipsilateral SN of controls (scr) and LAMP2A-deficient rats (L2), at 2 and 3 weeks post-injection. (A)*** *Nigral neurons in scr-injected rats displayed typical axons with intact mitochondria.* ***(D, E)*** *No cytoplasmic AVs were evident in scr- or L2-injected rats, at 2 weeks post-injection.* ***(C)*** *In contrast, accumulation of double or multi membrane AVs with storage material in degenerating processes of LAMP2A-deficient rats was detected mainly at 3 weeks.* ***(F)*** *AVs were detectable at the pericaryon of LAMP2A-deficient rats only 3 weeks post injection. Scale bars: 0.2-0.5 µm.*

### *D.5 LAMP2A down-regulation is accompanied by accumulation of AVs in the striatum as early as 2 weeks post-injection*

We subsequently examined whether such induction of macroautophagy is also occurring at the level of the nigrostriatal dopaminergic terminals. To this end, we have performed a similar ultrastructural analysis in the striatum of scr and L2 AAV-injected rats at 2 and 3 weeks following injection, utilizing Electron Microscopy (EM) with immune-gold labeling for GFP **(Fig. 6)**. LAMP2A down-regulation was accompanied by massive accumulation of AVs within nigrostriatal axons, already evident by 2 weeks post-injection. Multilamellar bodies, which are also of autophagic origin, also commonly appeared in the SN of L2-injected animals, at 2 weeks **(Fig. 6D)**. At 3 weeks

post-injection, the progressive accumulation of AVs in the striatum coincided with the degenerative areas **(Fig. 6G)**. Interestingly, AVs at early stages of autophagy pathway consisting of double membrane-bound vesicles were also observed within dopaminergic synaptic terminals of LAMP2A-deficient rats, both at 2 and 3 weeks post- injection **(Fig. 6F,I)** while such structures were absent in scr-treated controls **(Fig. 6A-C)**.

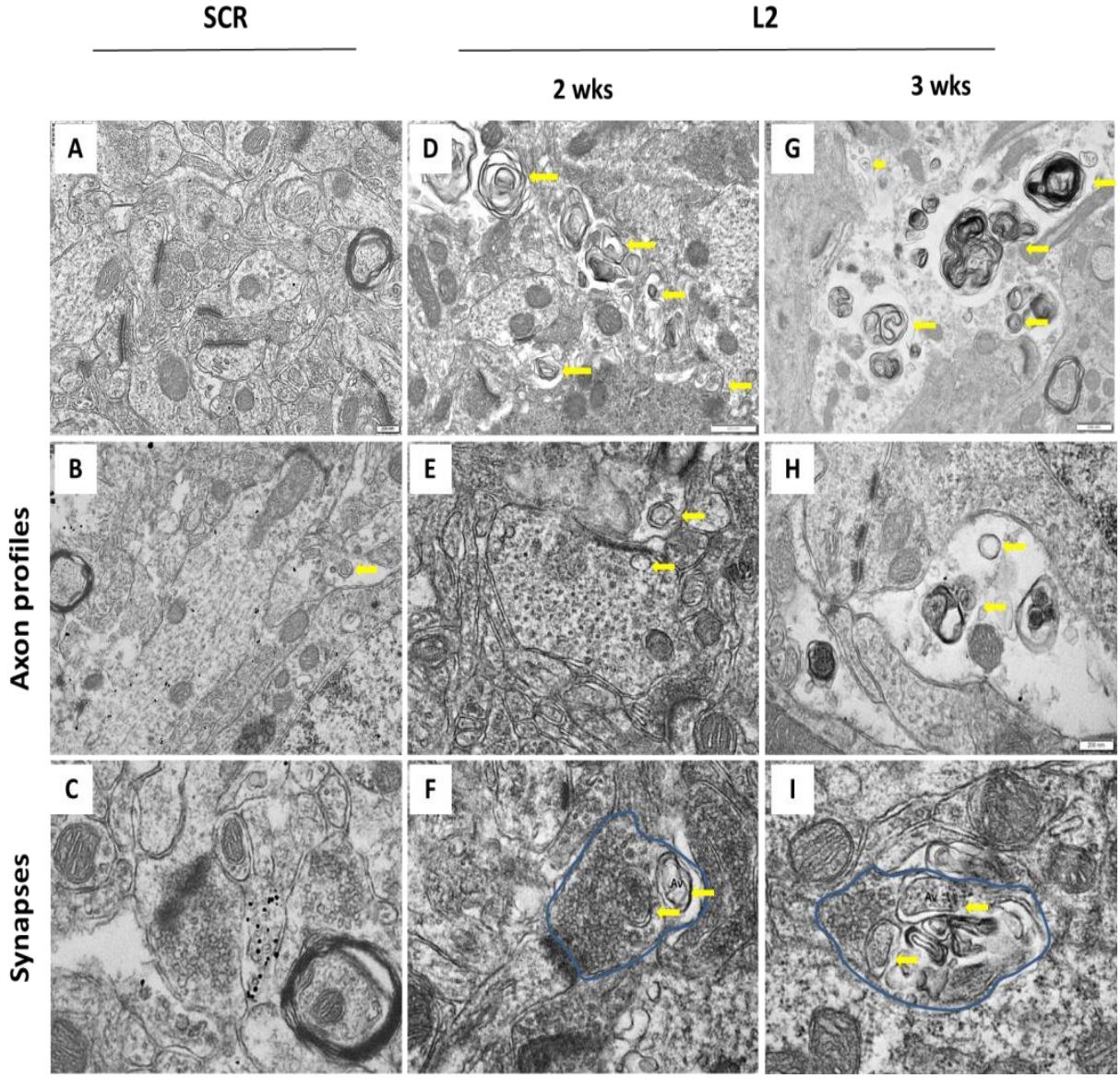

***Fig. 6: Representative electron micrographs with immunogold labeling for GFP of the ipsilateral striatum of controls (scr) and LAMP2A-deficient rats (L2), at 2 and 3 weeks post-injection. (A-C)*** *Nigral axons of scr-injected rats displayed typical morphological features with intact synaptic terminals.* ***(D, G)*** *Progressive accumulation of AVs and multilamellar bodies was observed in the striatum of LAMP2A-deficient rats compared with the scr- injected controls.* ***(E, H)*** *Electron micrographs at higher magnification showing axon profiles of LAMP2A-deficient rats containing AVs.* ***(F, I)*** *Electron micrographs at higher magnification showing progressive abnormal accumulation of AV-like structures within the synaptic terminals of L2-injected rats. Scale bars: 0.2-0.5 µm.*

### *D.6 LAMP2A down-regulation results in accumulation of early AVs in the synaptic terminals, at 3 weeks post-injection*

Given the observations of increased abundance of AV-like structures in the synaptic terminals of L2-deficient rats, synaptosomes were isolated from the striatum of scr and L2-injected rats at 3 weeks post injection, for electron microscopy and biochemical analysis, to further confirm whether AVs abnormally accumulate at synaptic nerve terminals. We initially performed electron microscopy analysis of our synaptosomal preparations that confirmed the enrichment of our preparations in intact synaptosomes, containing both pre- and post-synaptic membrane-bound elements (pre-synaptic vesicles and synaptic densities) occasionally bound together at the synapse **(Fig. 7)**.

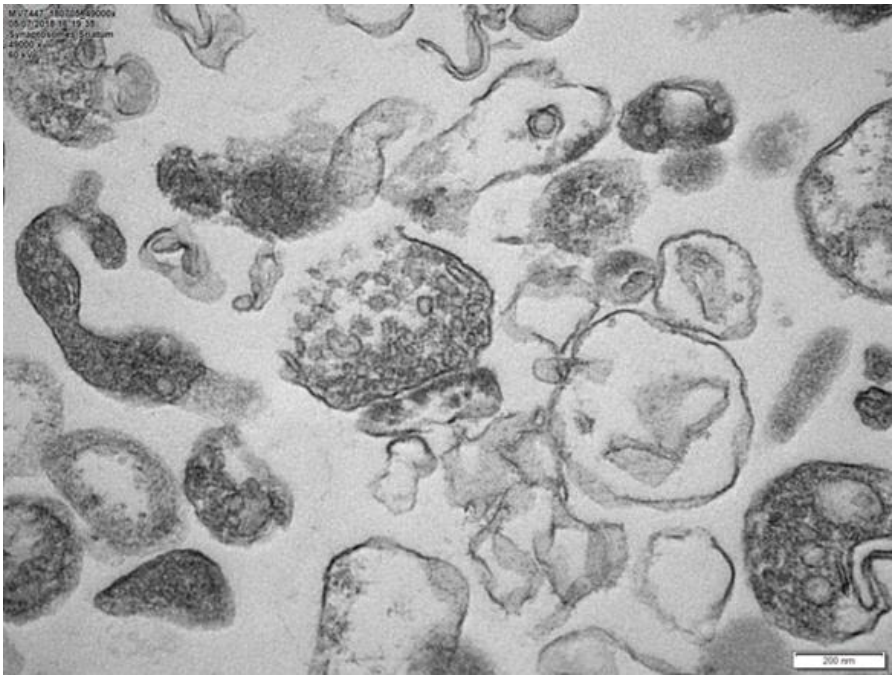

***Fig. 7: Electron micrograph of a synaptosomal preparation depicting a synaptosome with preserved pre-synaptic and post-synaptic element****. The presynaptic terminal with vesicles and the thick layer of the postsynaptic density (PSD) is shown.*

We subsequently obtained synaptosomal preparations from scr- and L2-injected rats at 3 weeks post-injection, to evaluate whether AVs accumulate in the pre-synaptic terminals of LAMP2A-deficient rats compared to controls **(Fig. 8)**. Our analysis, further confirmed that pre-synaptic striatal terminals of L2-injected animals are characterized by accumulation of AVs **(Fig. 8C-F)**, which were absent from scr-injected rats **(Fig. 8A-B)**. These AVs consisting of double membrane-bound vesicles contained undigested compacted organellar material, as well as synaptic-like vesicles probably representing initial stages of autophagy pathway, also known as phagophore **(Fig. 8D)**. Single membrane vesicles (arrowheads) were also observed, suggesting that these may represent autophagosomes with partially digested material and/or mature degradative forms of AVs (autophagolysosomes) **(Fig. 8D-F)**. These morphologically altered presynaptic terminals confirmed the induction of autophagy within the presynaptic compartment *and* may represent the initial stages of synaptic disruption and loss of synaptic integrity.

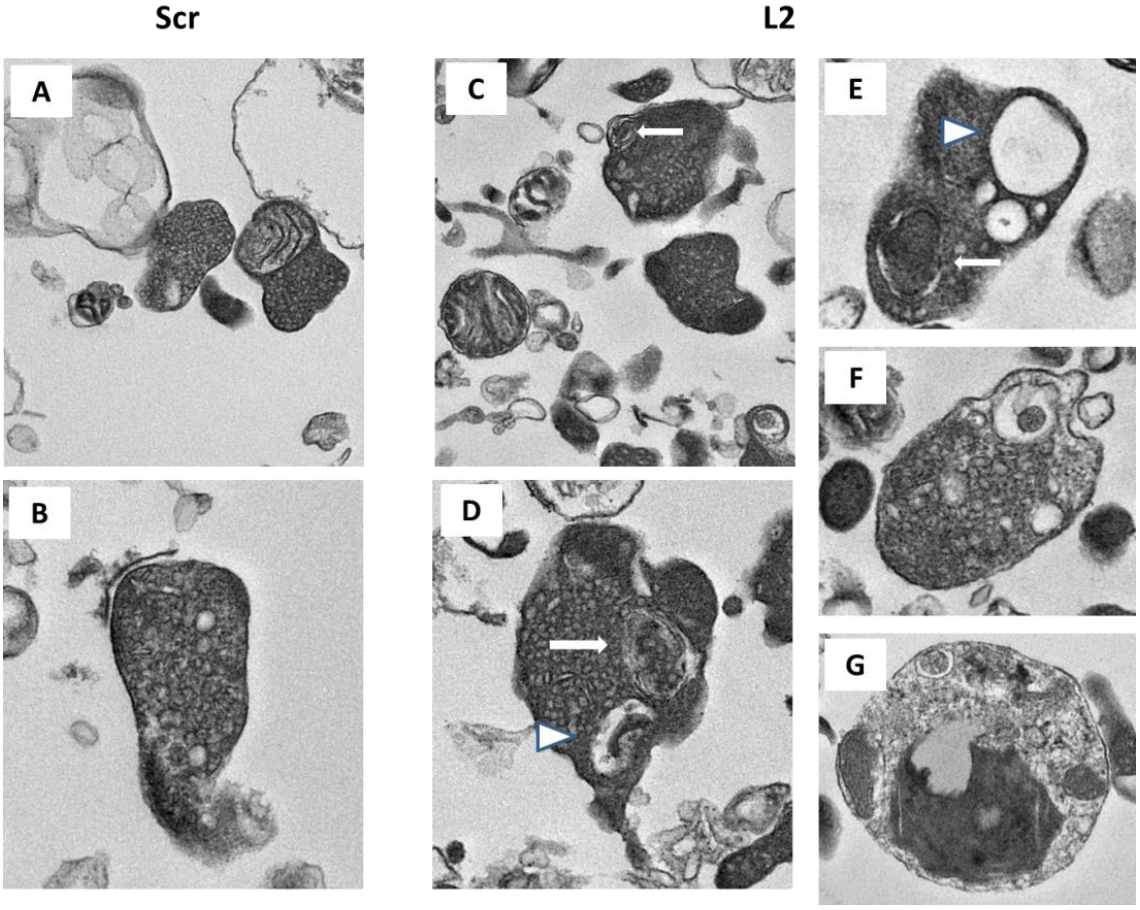

***Fig. 8: Representative electron micrographs of synaptosomal preparations of the ipsilateral striatum of controls (scr) and LAMP2A-deficient rats (L2), at 3 weeks post injection****. **(A-B)** Synaptic terminals of scr-injected rats containing increase abundance of normal synaptic vesicles and intact mitochondria, are shown. **(C-F)** Synaptic terminals of L2-injected rats with aberrant accumulation of autophagosome-like structures (arrow) indicating by the arrows are shown. **(D, E)**. Pre-synaptic terminals from L2-injected rats at higher magnification depicting a phagophore engulfing synaptic-like vesicles, as well as an autophagosome containing partially degraded material (arrowhead).* Scale bars: 0.2-0.5 µm.

We have also assessed the protein levels of the macroautophagic markers LC3I/II and SQSTM1/p62 in separate synaptosomal preparations derived from the contralateral (C) and ipsilateral (I) sites of scr- and L2-injected rats, with western immunoblotting **(Fig. 9)**. As shown in Fig. 9, no differences were observed in LC3 II levels between scr and L2-injected rats in the synaptosome-enriched preparations, but this likely reflects a sampling effect. The presynaptic marker synaptophysin and TUBG (tubulin) were used as marker for the synaptosomes and as loading control, respectively.

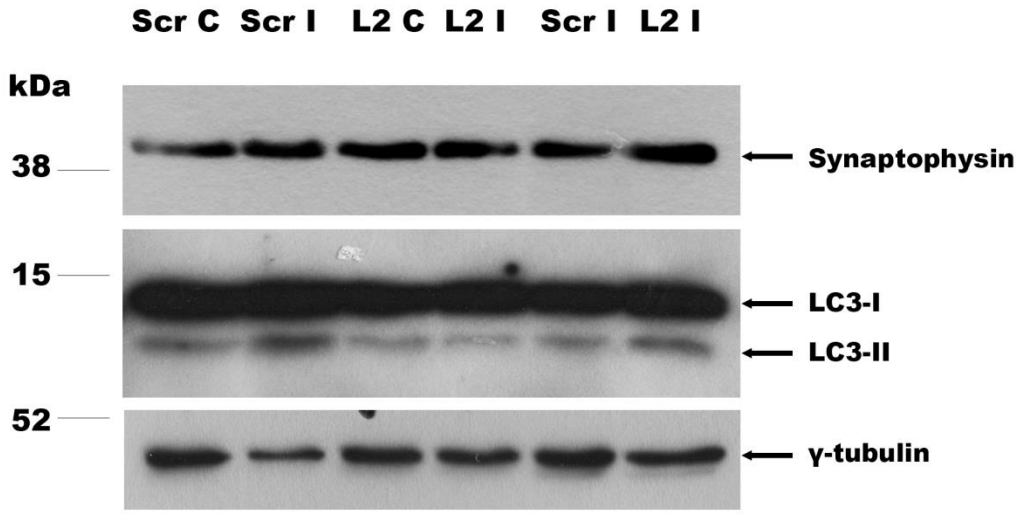


***Fig. 9: Representative western immunoblots in synaptosomes-enriched preparations derived from the contralateral (C) and ipsilateral (I) striata of scr and L2-injected rats, at 3 weeks post injection.*** *Western immunoblotting analysis for LC3-I, LC3-II, synaptophysin and TUBG (loading control) are shown.*

### *D.7 CMA deficiency is accompanied by increased ULK1 levels within GFP$^+$ transduced nigral neurons, at 3 weeks post injection*

It is well known that CMA and macroautophagy compensate for each other, but how they are linked together is incompletely understood (Kaushik et al. 2008; Wu et al. 2015). A very recent manuscript provides an interesting possibility, suggesting that ULK-1 is the key regulator linking these pathways. In this study, the authors reported that ULK-1, a key protein involved in autophagy initiation, promotes autophagosome–lysosome fusion, whereas phosphorylation of ULK-1 by PKCα prevents this event. They further show that phospho-ULK-1 at Ser423 is degraded by the CMA pathway, and that it prevents autolysosome formation and reduces macroautophagy upon its accumulation with CMA inhibition (Wang et al. 2018). To test the hypothesis that ULK1 could provide a link between macroautophagy and CMA in our *in vivo* model of CMA impairment, midbrain sections were immunostained with antibodies against TH (white), ULK-1 (red) and GFP (green) **(Fig. 10)**. Interestingly, we found that CMA impairment increased the levels of ULK-1 within L2-transduced nigral neurons at 3 weeks post-injection. Our results provide the first *in vivo* evidence that ULK-1 is a CMA substrate.

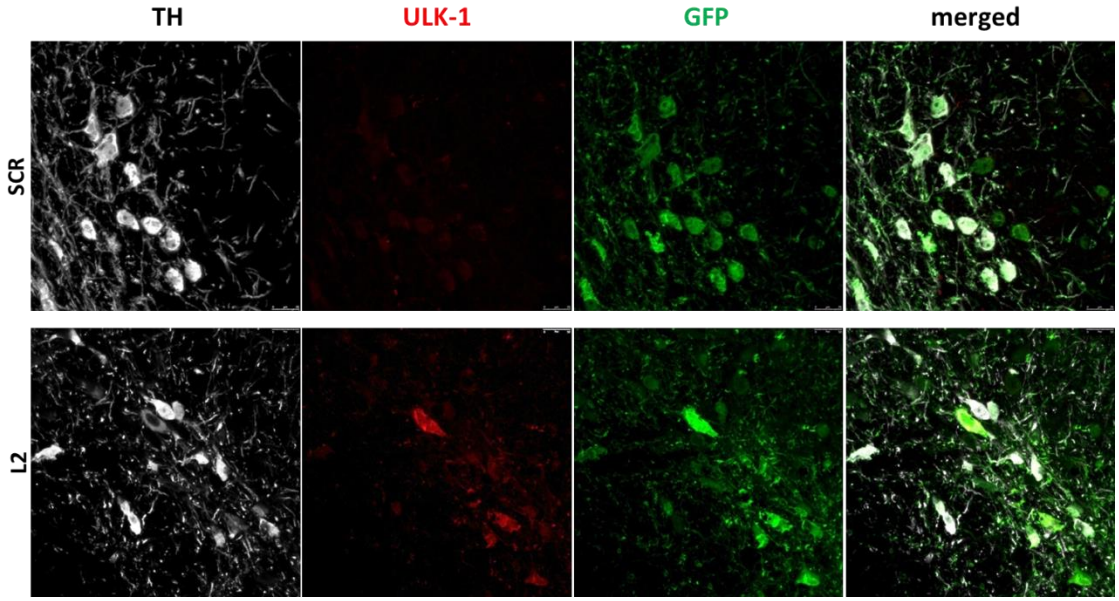


***Fig. 10: LAMP2A down-regulation is accompanied by increased ULK-1 levels within transduced nigral neurons, at 3 weeks post-injection.*** *Representative immunofluorescence images depicting ULK-1 levels within GFP$^+$ LAMP2A deficient nigral neurons, at 3 weeks post-injection Scale bar: 25 µm.*

### *D.8 LAMP2A down-regulation leads to impaired dopaminergic synaptic integrity, which is detected prior to nigral cell degeneration*

In order to evaluate whether the observed induction of macroautophagy in the nigrostriatal axis may have an impact on dopaminergic synaptic integrity, we have measured striatal levels of dopamine transporter (DAT), a transmembrane protein responsible for the reuptake of dopamine from the synaptic cleft and Bassoon, a multi-domain protein of the presynaptic active zone **(Fig. 11)**. The levels of DAT are considered to be a reliable marker of presynaptic dopaminergic terminal loss, while the levels of Bassoon correlate with synaptic function. At 3 weeks post-injection, a tendency for decreased DAT protein levels was observed in LAMP2A-deficient rats (0,73±0.11), compared with the control scr-injected rats (1,00±0,03). On the other hand, at the same time point the levels of the synaptic marker Bassoon were statistically reduced (0,61±0,27) compared with the control rats (1,00±0,01). No statistical significant differences were observed between L2 and scr-injected rats at 2 weeks post-injection **(Fig. 11)**.

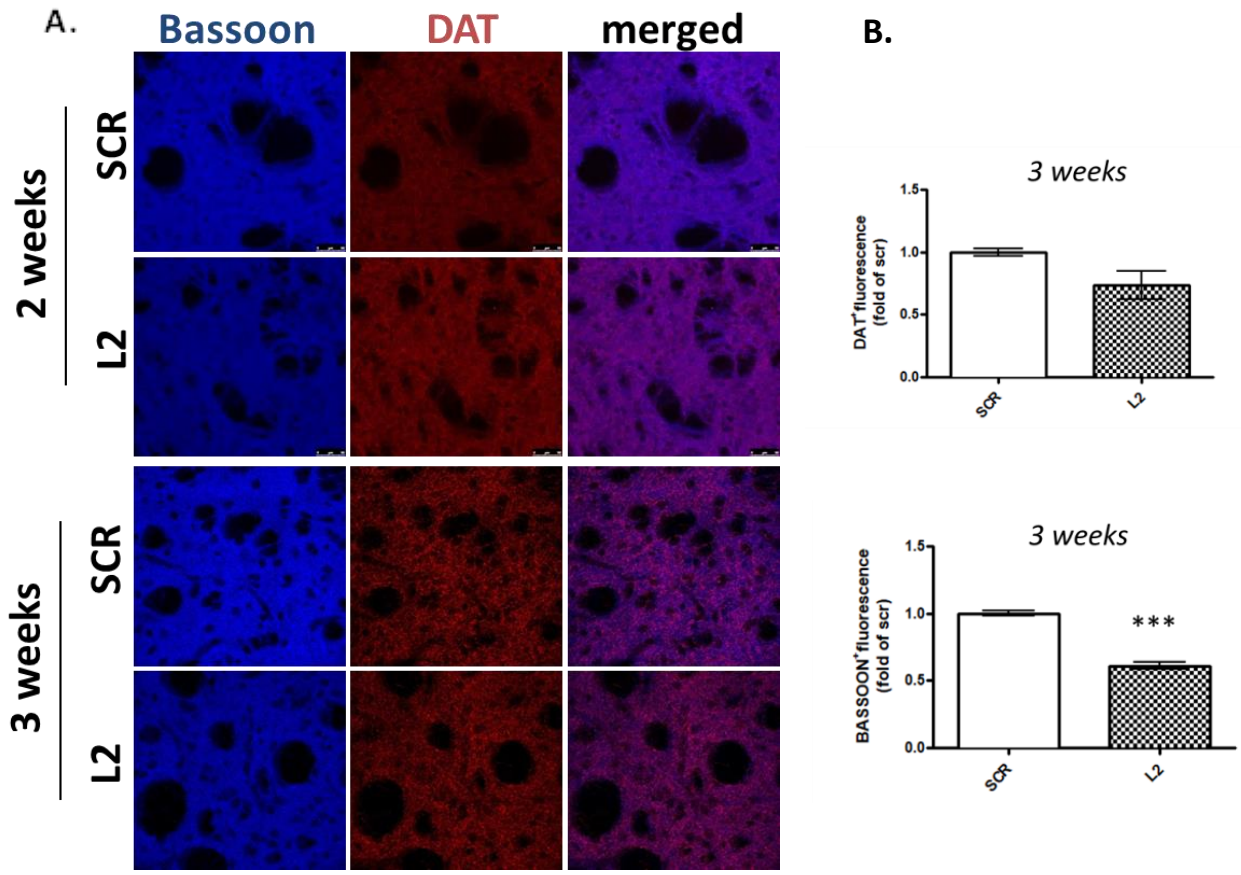

***Fig 11: CMA impairment leads to impaired synaptic integrity of the nigrostriatal dopaminergic terminals in LAMP2A-deficient rats, at 3 weeks post-injection.*** **(A)** Representative immunofluorescence staining from striatal sections with antibodies against Bassoon and Dopamine transporter (DAT) at 2 and 3 weeks post-injection are show. Scale bar: 50 µm. **(B)** Quantifications of Bassoon and DAT positive fluorescence at 3 weeks post-injection are shown (***, p=0,0003; n = 3 animals/group, t-test). No statistically significant differences were observed at 2 weeks post-injection (data not shown).

Furthermore, we evaluated the effect of LAMP2A silencing on the integrity of the nigrostriatal axis. We utilized densitometric evaluation of the neuronal terminals in the injected and the non-injected striatum of the scr- and L2-injected rats, at 2 and 3 weeks post-injection. Densitometric analysis of dopaminergic fiber density in the striatum by TH immunoreactivity revealed no statistically significant differences between all groups, indicating that the observed synaptic alterations occur prior to degeneration **(Fig. 12)**.

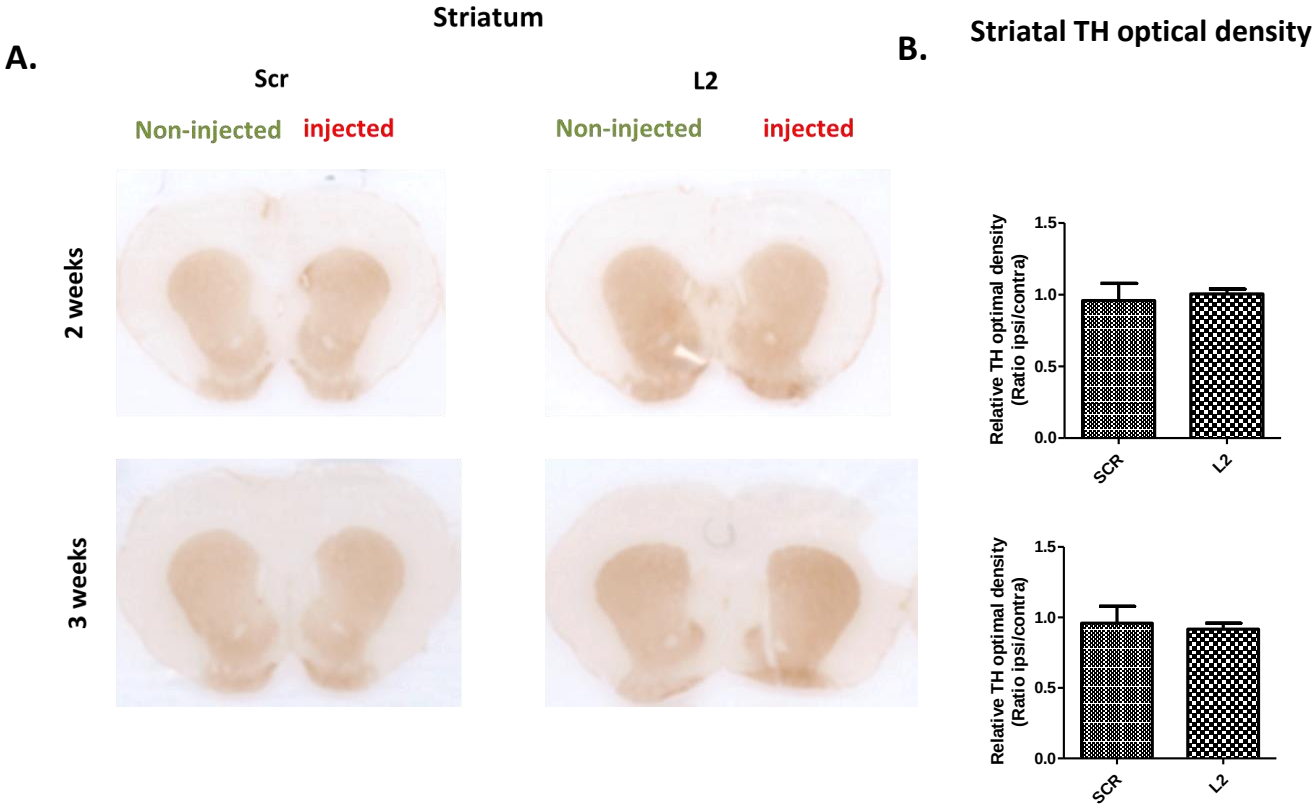


***Fig. 12: LAMP2A-deficiency is not accompanied by significant alterations in TH$^+$ immunoreactivity in the injected striata, at 2 and 3 weeks post-injection.*** **(A)** Representative striatal images of animals injected with scr and L2 recombinant AAVs,

at 2 and 3 weeks post-injection. **(B)** Densitometric analysis of dopaminergic fiber density in the striatum of scr- and L2- injected rats by TH immunoreactivity (n=5)

### *D.9 Increased astrogliosis and microgliosis throughout the nigrostriatal axis in LAMP2A-deficient rats, at 3 weeks post-injection*

Finally, we explored whether CMA inhibition via LAMP2A silencing was accompanied by astro- and micro-gliosis in the nigrostriatal axis, considering that possible activation of these glial cells may mediate the neurodegenerative effect observed at the later time points. The neuroinflammation has long been considered a downstream response to the death of dopaminergic neurons (ref). However, evidence is building to suggest that glial cells have an initiating role in the neurodegenerative processes. Therefore, we immunostained midbrain and striatal sections from scr- and L2-injected animals with the astrocytic marker GFAP (glial fibrillary acidic protein), and microglia marker AIF1/IBA-1. Representative images of GFAP immunostaining in the striatum and the substantia nigra (SN) of LAMP2A deficient rats are shown in **Fig. 13**. A statistically significant increase in the $GFAP^+$ signal density was already detected by 2 weeks post-injection in LAMP2A-deficient rats (1,25±0,07), as compared to the scr-injected ones (0,77±0,22), only in the striatum (Fig. 12A). No statistically significant differences were observed between L2-(0,69±0,1) and scr-(1,00±0,11) injected rats in the SN **(Fig. 12B)**. At 3 weeks post-injection, $GFAP^+$ astrocytes were found increased in both the striatum and the SN (2,88±0,59, 2,49±0,88, respectively) of L2-injected rats, as compared to the scr control ones (1,00±0,15, 1,00±0,08, respectively).

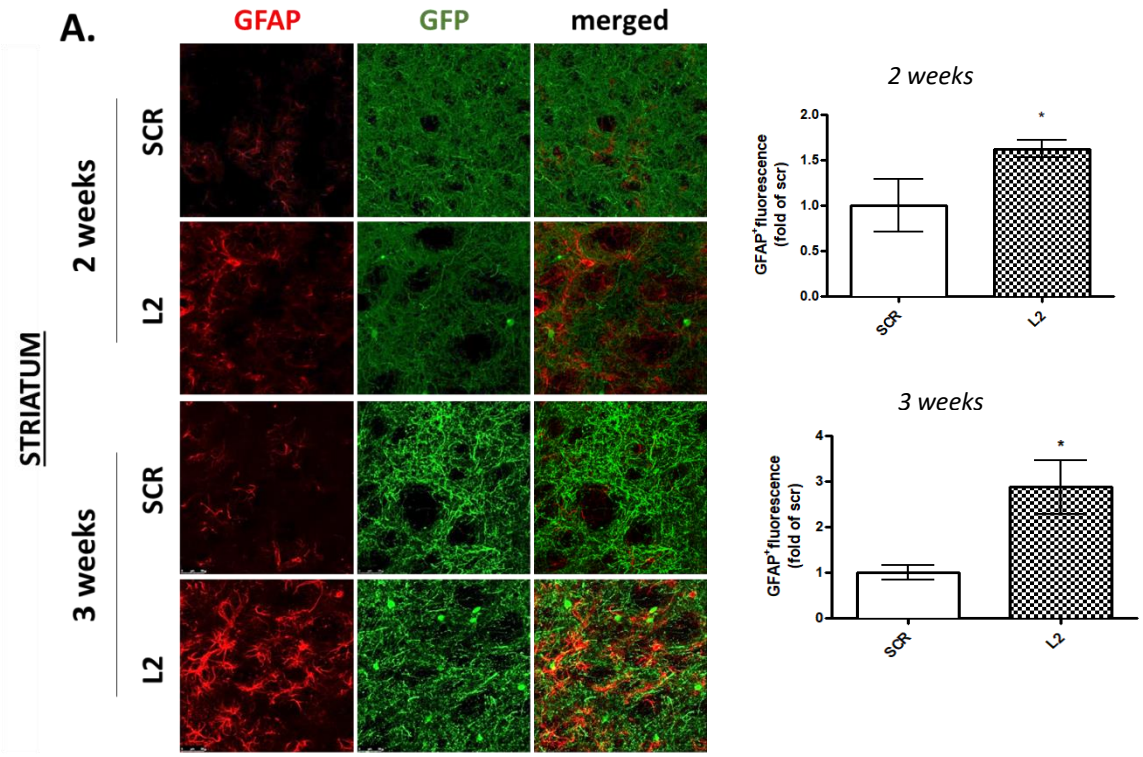
A.
GFAP
GFP
merged
STRIATUM
2 weeks
3 weeks
SCR
L2
2 weeks
3 weeks
GFAP+ fluorescence (fold of scr)
SCR
L2

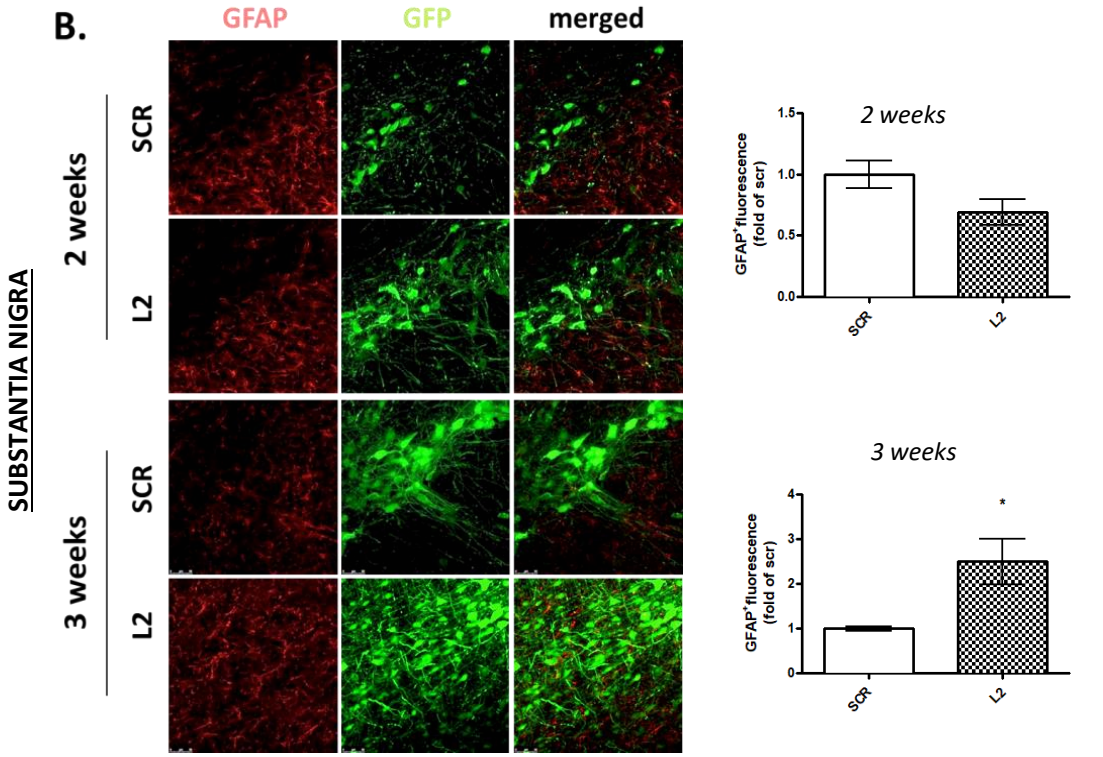
B.
GFAP
GFP
merged
SUBSTANTIA NIGRA
2 weeks
3 weeks
SCR
L2
2 weeks
3 weeks
GFAP+ fluorescence (fold of scr)
SCR
L2

**Fig. 13: LAMP2A deficiency is accompanied by robust astrogliosis in transduced nigral neurons and striatal terminals.** (A, B) Representative immunofluorescence images of GFAP$^+$ astrocytes in the striatum (A) and in the vicinity of GFP$^+$ nigral neurons (B), at 2 and 3 weeks post-injection are shown in the left panels. Scale bar: 50 µm. Quantifications of GFAP+ fluorescence of striatal and ventral midbrain tissues are shown in the right panels (*, $p < 0.05$; n = 3 animals/group, t-test).

Representative images of AIF1/IBA1 immunostaining in the striatum and the substantia nigra of LAMP2A-deficient rats are shown in **Fig.14**. Likewise, a statistically significant increase in IBA-1 immunoreactivity was observed in the L2-injected striatum and the substantia nigra of L2-injected rats, compared with the control rats.

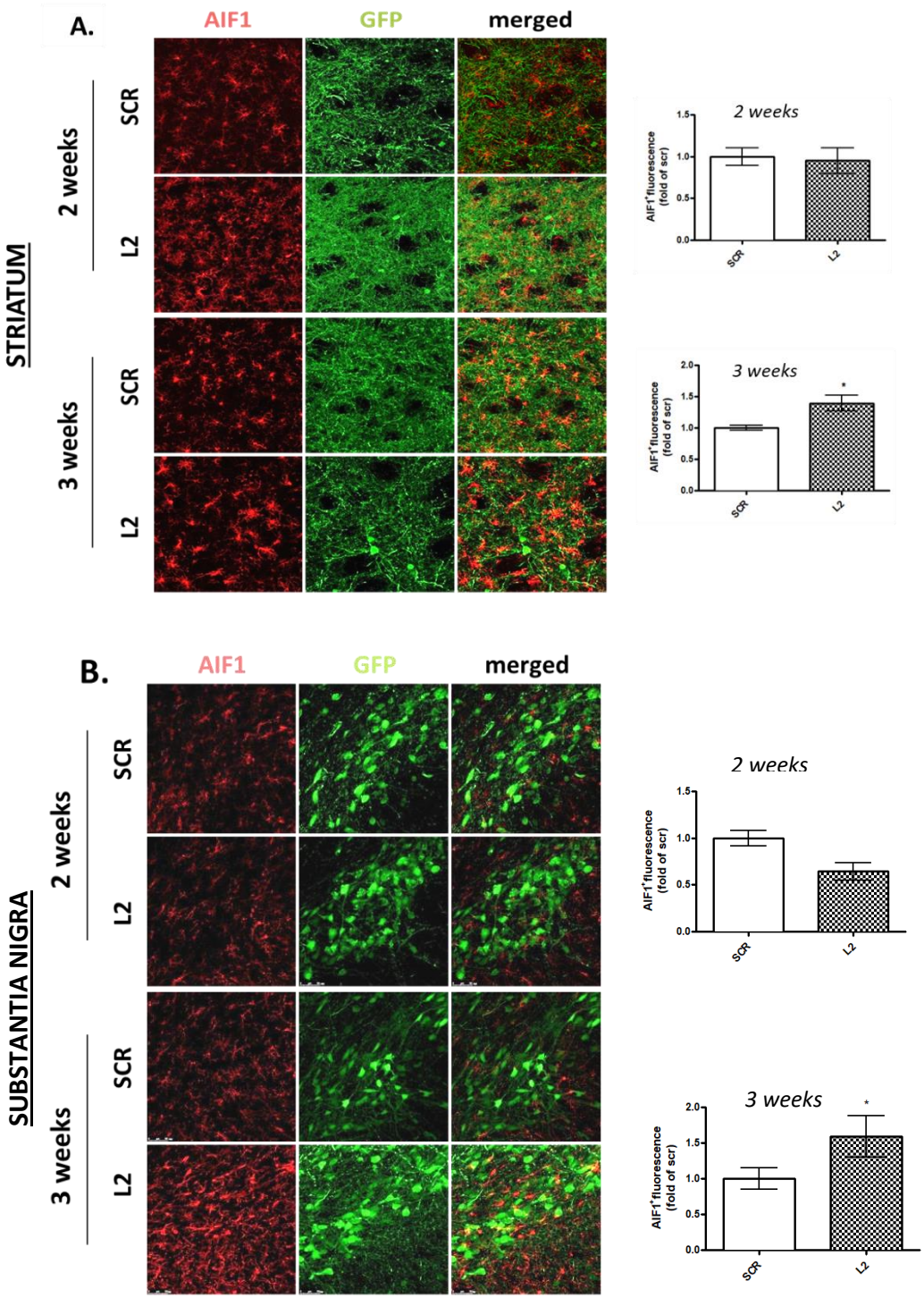

***Fig. 14 LAMP2A deficiency is accompanied by robust micro-gliosis in transduced nigral neurons and striatal terminals.*** **(A,B)** Representative immunofluorescence images of $AIF1^+$ microglia in the striatum **(A)** and in the vicinity of $GFP^+$ nigral neurons **(B)**, at 2 and 3 weeks post-injection are shown in the left panels. Scale bar: 50 µm. Quantifications of $AIF1^+$ fluorescence of striatal and ventral midbrain tissues are shown in the right panels (*, $p < 0.05$; n = 3 animals/group, t-test). Scale bar: 50 µm.

# E. Discussion

A growing body of evidence demonstrates that imbalanced induction of autophagy leads to neurodegeneration in the central nervous system (Kiriyama and Nochi 2015; Menzies et al. 2017). Dystrophic axons/neurites containing accumulated autophagosome-like structures have frequently been observed in several injury models and in human brains derived from patients exhibiting neurological diseases, such as AD (Nixon et al 2005, Yu et al. 2005), PD (Dehay et al.2010, Alvarez-Erviti L et al. 2010) and HD (Shibata M, et al. 2006). In the current project, we sought to uncover the contribution of macroautophagy in the axonal degeneration we observe upon inhibition of the CMA pathway via down-regulation of its rate-limiting step, the LAMP2A receptor, in the rat nigrostriatal system. We were especially interested in the phenomenon of retrograde axonopathy, as this resembles features seen in PD and other neurodegenerative conditions. Our previously reported data show that CMA inhibition in the rat substantia nigra, induced through the injection of AAVs encoding shRNAs selectively targeting the LAMP2A receptor, led to a profound degeneration of the nigrostriatal axis, that was already pronounced at the level of the dopaminergic terminals at 4 weeks, and only became significant at the level of nigral cell bodies at 8 weeks post-injection. At the same time point (8 weeks), a marked accumulation of autophagic vacuoles and biochemical indices suggestive of enhanced productive macroautophagy in the nigral cell bodies of the remaining dopaminergic neurons were detected (Xilouri et al. 2016).

Such data suggested that the observed likely excess compensatory activation might be linked to the dopaminergic axonal degeneration. In order to elucidate the contribution of macroautophagy induction in this model, we have analyzed indices of macroautophagy at the earlier time points of 2 and 3 weeks post-injection, when no overt axonal neurodegeneration, is evident. We have initially analyzed by immunofluorescence microcopy the levels of the macroautophagy markers LC3 and SQSTM1/p62 within $GFP^+$ transduced nigral neurons, at both time points. Our analysis revealed an increase in LC3 (**Fig. 3**) and a decrease SQSTM1/p62 (**Fig. 4**) protein levels at 3 weeks post-injection, suggesting a "productive" over-activation of macroautophagy. The analysis of the striatum with confocal microscopy was not informative, due to the difficulty in detecting positive LC3 or SQSTM1/p62 signal in $GFP^+$ nigrostriatal axons (data not shown). For this reason, the analysis in the striatal tissues was restricted mostly to electron microscopy analysis, which represents the most reliable method for the detection of macroautophagy activation. Towards this direction, we performed ultrastructural analysis of the injected substantia nigra and striatum, at 2 and 3 weeks post-injection. EM-analysis of the $GFP^+$ nigral neurons revealed an accumulation of numerous AVs with storage material in the LAMP2A-

deficent neurons, compared to the scr-controls(**Fig. 5**). The number of AVs in the perikarya of, LAMP2A-deficient was relatively small compared with their abundance in most affected neurites, consisting with the decreased p62 levels, which suggested efficient fusion of AVs with the lysosomes and subsequently enhanced autophagic flux.

Most importantly, we found that LAMP2A down-regulation was accompanied by accumulation of AVs in the striatum as early as at 2 week post-injection (**Fig. 6**). A number of these vesicles contained multilamellar membranous structures, another variant of AVs (Hornung et al., 1989; Hariri et al., 2000; Nixon et al., 2005; Borsello et al., 2003). Interestingly, a striking number of AV-like structures were retained within the presynaptic terminals of LAMP2A-deficint animals, relative to that of scr controls, some of which often containing subcellular organelles, such as mitochondria or synaptic vesicles already by 2 weeks post injection. To further investigate the compartmentalized regulation of autophagy in LAMP2A-deficient rats, as a complementary approach, we performed electron microscopy analysis in purified synapse-enriched synaptosomes from scr and L2 injected rats. The electron micrographs in **Fig. 8** illustrate the presence of early and late AVs in the synaptic terminals of LAMP2A-deficient rats, compared to the scr-injected control rats. Interestingly, these early AVs often contained engulfed synaptic vesicles. Taken together, our results suggest that CMA impairment induces macroautophagy pathway activation in the presynaptic compartment of nigrostriatal terminals as early as 2 weeks post injection, whereas such phenomena are detected later in the nigral cell bodies (3 weeks post-injection).

A close crosstalk between CMA and macroautophagy has been reported in many cellular systems, as experimental blockage of one of them results in compensatory upregulation of the other. Massey et al. (2006) were the first to report that specific CMA inhibition may lead to compensatory activation of macroautophagy. Further, this effect has been reported by us in vitro (Vogiatzi et al.2008) and by others in vivo, in LAMP2-deficient mice (Rothaug et al. 2015; Tanaka et al. 2000). A potential molecular link of CMA to macroautophagy could be provided by ubiquilin, which has been shown to be a substrate for both CMA and macroautophagy and can promote macroautophagy (Rothenberg et al. 2010). More recently Wang et al. provided evidence that ULK1 is the key regulator linking these pathways and suggested that phosphorylation of ULK1 at Serine 423 targets it for CMA-dependent degradation (Wang et al. 2018). In particular, they found that active PKCα, which represents a high nutrient condition for cells, inhibits the late stages of autophagy not only through phosphorylation of LC3, but also through phosphorylation of ULK1. With sufficient nutrients, ULK1 is phosphorylated and degraded by the CMA pathway, as a response of the cell to reduce macroautophagy. Such data imply that upon CMA blockade, the removal of ULK1 is impaired thus leading to excessive activation of macroautophagy.

In the present thesis we have investigated whether a similar effect on Ulk1 levels can be detected in the LAMP2A-deficient rats, at the time point of 3 weeks when the massive accumulation of AVs in both nigra and striatum is evident. Importantly, our results show that indeed ULk1 levels are found increased in $GFP^+$ nigral cells bodies of LAMP2A-deficient rats, compared to the control rats **(Fig. 10)**, providing the first in vivo evidence of CMA-dependent regulation of Ulk1 levels.

Given the uniqueness of the neuronal structure encompassing a distinct cell soma with dendrites and axons with presynaptic regions, neuronal autophagy exhibits a high degree of compartmentalization within the neuron (Maday and Holzbaur, 2016). Recent studies from several groups provide strong evidence that AVs are predominantly generated in distal axons, and undergo retrograde transport toward the cell soma for lysosomal proteolysis (Vanhauwaert, R., et al. 2017; Cheng et al., 2015a; Fu et al., 2014; Lee et al., 2011a; Maday and Holzbaur, 2014; Maday et al., 2012). In particular, a recent study reported that two distinct populations of AVs can be found in neurons; one derived from the axon and synapse and a second generated in the cell body (Maday and Holzbaur, 2016). They also showed that these axon-generated AVs form continuously in distal tips and contain cargoes derived from synapses (Maday et al., 2012; Maday and Holzbaur, 2014, 2016; Wang et al., 2015). Upon formation, AVs or autolysosomes are transported via retrograde motion by dynein along microtubules to the cell body, where mature lysosomes are mainly located (Hollenbeck, 1993; Cheng et al. 2015). Thus, proper macroautophagy function requires efficient transport of the AVs formed in distal parts of the axon, to the cell soma; any impairment of such conveyance may lead to accumulation of AVs in the areas formed. In addition, macroautophagy has already been shown to contribute in the regulation of postsynaptic receptors, such as GABAa (Rowland et al. 2006) and AMPA (Shehata et al. 2012) receptors. Furthermore, Nikoletopoulou et al. (2017) found that postsynaptic scaffold proteins, namely PICK1, PSD-95, and SHANK3, constitute substrates for autophagic-dependent degradation. However, it is still unclear whether the turnover of the presynaptic proteins is regulated by the same pathway. Such findings are in agreement with the seminal report by Holtzman in 1971, who predicted that the turnover of recycled synaptic vesicles might require lysosomes. Emerging evidence suggests that autophagy facilitates the homeostasis of the synapse serving local functions related to synaptic morphology and function; therefore imbalanced induction of macroautophagy may lead to disruption of the presynaptic homeostasis.

Another important aspect of the presynaptic proteostasis is the maintenance of synaptic vesicle (SV) pools within synaptic buttons. Such pools are necessary to support the sustained release of neurotransmitters by maintaining a local reservoir of SV-associated proteins and membranes to facilitate vesicle recycling (Denker et al, 2011a, 2011b). Presynaptic autophagy has been found to mediate the degradation of

SVs. Notably, Hernandez and colleagues found that in dopaminergic neurons, induced autophagy can reduce the kinetics of dopamine release and synaptic vesicle numbers and subsequently can alter presynaptic structure, while chronic macroautophagy deficiency via Atg7 knockout increased dopamine release and axonal size (Hernandez et al. 2012). Interestingly, Binotti et al. (2015) found that Rab26 mediates selective targeting of SVs to the autophagy pathway hinting at a potential parallel synaptic trafficking pathway that recycles older vesicles and their associated proteins via autophagy as well.

Synaptic proteins such as Endophilin A (EndoA) (Vanhauwaert et al. 2017) and Synaptojanin-1 (Soukup et al. 2016) were reported to intersect with the autophagy machinery to promote synaptic autophagy. Another recent study demonstrated that the presynaptic protein Bassoon has a crucial role in this process, by actively inhibiting macroautophagy. Bassoon is known to organize the presynaptic active zone and to regulate the release of SVs (Ackermann et al.2015). More recently, Okerlund et al. (2017) reported that Bassoon negaively regulates the macroautophagy pathway in hippocampal neurons, by binding to Atg5, an E3 ubiquitin ligase-like enzyme essential for the attachment of LC3 to AVs. Loss of Bassoon triggered the induction of macroautophagy within the presynaptic compartment, which was accompanied by a progressive loss of the SV pool, suggesting that macroautophagy is responsible for the degradation of SVs or of their components. In our model of CMA deficiency, the decreased protein levels of Bassoon at 3 weeks post-injection (**Fig. 11**) were associated with the marked induction of macroautophagy and the subsequent degradation of SVs in the nigrostriatal terminals, as determined by electron microscopy. Such findings demonstrate that excessive induction of macroautophagy, occurring probably as a secondary effect to compensate for defective CMA, is responsible for the impaired synaptic integrity. Whether the loss of Bassoon we have observed plays a contributory role to the induction of macroautophagy in this model remains to be determined.

In order to assess whether the synaptic changes, detected mainly at 3 weeks post-injection, were related to the degeneration of the nigrostriatal axis, we assessed the integrity of dopaminergic striatal terminals using immunohistochemistry with DAT and TH in striatal sections (**Fig 11** and **12**). Our results did not reveal any statistically significant differences between LAMP2A-deficient rats compared with controls, suggesting that the observed presynaptic dysfunction occurs before overt neurodegeneration (**Fig. 12**). It has to be noted though that on EM we did identify at 3 weeks post-injection discrete areas of axonal degeneration; obviously, the extent of this emerging axonal degeneration was not sufficient to be detected at the level of all the striatal terminals. In association with these alterations in axonal morphology, an inflammatory response was identified in the striatum but not in the nigra of LAMP2A-deficient rats, as demonstrated by the statistically significant increased levels of GFAP,

even at 2 weeks post-injection (**Fig. 13**). LAMP2A silencing was further accompanied by astro- and micro-gliosis along the whole nigrostriatal axis at 3 weeks post-injection, suggesting that these glial cells are recruited early in the pathological cascade of events leading to dopaminergic neurodegeneration. The pathway through which glial cells sense the emerging axonal degeneration and their possible role in influencing such degeneration is a very interesting subject for future study.

We have previously reported that already by 4 weeks, there was a profound loss of nigrostriatal axons, while the ones that were remaining displayed a beaded pattern with axonal swellings, indicative of ongoing neuritic degeneration (Xilouri et al, 2016). In the *"dying-back"* hypothesis of PD-like neurodegeneration, the pathological cascade occurs initially at the level of axonal innervation in the striatum, which in turn causes cytotoxicity at the level of the dopaminergic nigral cell bodies (Burke et al. 2012). This is in accordance with our observations of significantly reduced striatal dopamine content at the 4 week time-point, where no statistically significant loss of dopaminergic cell bodies is observed. In this model, we have also noted other key features that occur in PD, such as cell body accumulation of alpha-synuclein-positive puncta that co-localized with ubiquitin, an induction of the formation of AVs in the nigra, a pronounced inflammatory reaction, and a motor phenotype reflecting the ipsilateral nature of the lesion (Xilouri et al, 2016). This indicates that initial CMA dysfunction in nigral neurons causes axonal degeneration, which, over time, results in severe cytotoxicity at the level of the substantia nigra. Therefore, by inhibiting CMA *in vivo*, we have succeeded in modeling cardinal aspects of PD at the level of the nigrostriatal axis.

In spite of the importance of axonal degeneration in PD and other neurodegenerative disorders, little is known of the underlying mechanisms. It is noteworthy that research on neurodegenerative diseases also indicates that not neuronal loss but synaptic changes are of importance in disease pathology (Burke and O'Malley, 2013, Soukup et al., 2013). Accumulating evidence supports the notion that PD, like AD, can be considered a synaptopathy (Plowey and Chu, 2011, Cheng et al., 2010), where failure of the synapse precedes neuronal dysfunction and eventual loss of the neuron (Selkoe, 2002; Oddo et al., 2003; Gouras et al., 2010). Due to early appearance of AVs within presynaptic terminals in our model, it is tempting to speculate that there is a causative relationship between induction of macroautophagy and neurodegeneration. Beyond PD, studies have also linked dysfunctional macroautophagy to synaptic pathology observed in many neurodegenerative conditions (Yoshimitsu and Hiromi 2015). Terry et al. (1991) has suggested that loss of synapses is the major correlate of AD-linked dementia. Synaptic dysfunction, accompanied by an autophagic stress-related phenotype, has been reported in the hippocampus of young AD model mice [Sanchez-Varo et al. 2012; Tammineni et al. 2017) and in postmortem brains from AD patients (Nixon et al. 2007). In this setting,

macroautophagy seems to be impaired due to alterations of the endo-lysosomal pathway, which impaired the fusion of autophagosomes with the lysosomes (Boland et al. 2008).

Regarding PD pathogenesis and synaptic alterations, the most common mutation in the LRRK2 protein, the pathogenic G2019S mutation, (Trinh et al. 2014) was reported to drive alterations in synaptic autophagy. In G2019S-LRRK2 transgenic mice increased abundance of AVs has been observed within synaptic terminals in cerebral cortex (Ramonet et al. 2011). More recently, Soukup and colleagues (2016) reported that LRRK2-dependent phosphorylation of EndoA at serine 75, shown previously to occur at the synapse (Matta et al., 2012; Arranz et al., 2015), is required for the induction of macroautophagy at Drosophila synapses. They also showed that the balance of EndoA phosphorylation affects neuronal survival, as deregulation of the EndoA phosphorylation state is accompanied by dopaminergic neuron degeneration. Therefore, LRRK2 dysregulation in PD seems to drive alterations in synaptic macroautophagy, starting a cascade leading to synaptic defects in PD. Synaptic loss is an early and major feature of the brain pathology induced by prion diseases as well (Fuhrmann M, et al. 2007). Prion infection induces the accumulation of AVs within synaptic terminals in various brain regions of infected hamsters and mice (Liberski et al. 2011). Autophagosomes were also found within damaged synapses in brain biopsies, derived from patients with prion disease (Sikorska et al. 2004). In line with these, our results suggest that these morphologically altered presynaptic terminals occurring prior to evident neurodegeneration may represent the initial stages of synaptic disruption and loss.

To sum up, this study has shown that induction of macroautophagy within the synaptic terminals of LAMP2A-deficient rats represents an early phenomenon occurring prior to dopaminergic degeneration. While macroautophagy may be essential in the maintenance of axon homeostasis, these data raise the intriguing possibility that the compensatory induction of productive macroautophagy may have deleterious consequences. The appearance of autophagic-related structures in dying neurites has led to the initial hypothesis that macroautophagy may play a causative role in the neuritic damage or degeneration induced by inhibition of CMA. In particular, as excessive autophagy can lead to excessive degradation of cell components and neuronal cell death (Button et al. 2015, Kroemer et al.2008, Lee et al. 2009), we speculate that uncontrolled induction of macroautophagy may contribute to the clearance of the synaptic proteins and receptors and thus underlie the synaptic pathology observed in our model. Thus, blockade of macroautophagy may represent a neuroprotective strategy. Towards this notion, a number of studies have also suggested that axonal degeneration can be suppressed by inhibition of macroautophagy. Induction of macroautophagy, characterized by an increase in autophagosome synthesis, is detected in both neurotoxin and physical injury

(axotomy) models. In particular, excess induction of productive macroautophagy, occurring secondary to diminished Akt signaling, has been implicated in axonal degeneration induced by axotomy or striatal injections of 6-OHDA, a neurotoxin-based PD model. Conditional deletion of the essential autophagy gene Atg7 in adult mice achieved striking axonal protection in these acute models of retrograde degeneration (Cheng et al. 2011), suggesting that macroautophagy may in fact contribute to axonal degeneration. Consistent with the *in vivo* observations, Yang and colleagues reported in several *in vitro* models of injury that both pharmacologic and genetic disruption of autophagy signaling protected from axonal degeneration (Yang et al., 2007). In G2019S-LRRK2-transfected SH-SY5Y cells, it was suggested that macroautophagy contributed to the progression of neuritic degeneration, as inhibition of macroautophagy via siRNA knockdown of LC3 or Atg7 reversed the mutant LRRK2-induced neurite retraction, whereas macroautophagy stimulation with rapamycin potentiated these effects (Plowey et al., 2008). Other interventions aiming at inhibition of macroautophagy, such as phosphorylation of LC3, also prevented mutant LRRK2-mediated neurite retraction in primary cortical neuronal cultures (Cherra et al., 2010). These findings indicate that excessive removal of mitochondria could be one of the contributing factors for dendritic retraction. We have also previously shown that in the rat primary cortical neurons and human differentiated SH-SY5Y cells, CMA inhibition conferred by aberrant alpha-synuclein overexpression lad to a compensatory induction of the process of macroautophagy and cell death. Interestingly, pharmacological and molecular macroautophagy inhibition exerted a protective effect in both models, further supporting a neurotoxic role of excessive macroautophagy induction (Xilouri et al. 2009).

Based on the aforementioned findings, in future experiments we seek to determine whether the concomitant down-regulation of macroautophagy through conditional knock out of Atg5 in the substantia nigra, may exert a protective effect against CMA inhibition. A potential pitfall may be that inhibition of macroautophagy via Atg5 knockdown may itself lead to axonal degeneration. Indeed, it has been reported that *in vivo* depletion of the Atg5 gene in the neural lineage provokes progressive neurodegeneration phenotype starting at 3 weeks of age (Hara et al 2006). However, similar experiments in the nigrostriatal system have shown that axons are preserved even for a period of two months of Atg7 depletion, and in fact are enlarged and appear to have enhanced properties, likely due to the lack of macroautophagy-dependent attrition of axonal and synaptic components; at later time points, Atg7-deficient nigrostriatal terminals do start to degenerate as well, however this is beyond our experimental window (Hernandez et al. 2012; Inoue et al. 2013). Therefore, we believe that in the time frame of our experiments axonal processes will be preserved in Atg5-deficient neurons.

If successful in showing that excess macroautophagy induction is responsible for axonal degeneration in this model, this would be an important finding for many reasons: ***a)*** It would decipher a pathway for axonal degeneration that may be relevant to a number of neurodegenerative conditions, ***b)*** It would provide an *in vivo* example where excess macroautophagy may be detrimental, and provide a note of caution for therapeutic trials attempting to augment macroautophagy for the treatment of neurodegenerative conditions, ***c)*** It would provide an example of the cross-talk between protein degradation pathways, in which excess compensatory mechanisms may be detrimental, and ***d)*** It would help decipher the mechanisms through which CMA dysfunction in the brain, as appears to occur in PD, may lead to neurodegeneration.

# F. References


**Ackermann, F**., Waites, C. L., & Garner, C. C. (2015). Presynaptic active zones in invertebrates and vertebrates. *EMBO reports*, *16*(8), 923-938.

**Agarraberes, F. A**., & Dice, J. F. (2001). A molecular chaperone complex at the lysosomal membrane is required for protein translocation. *Journal of cell science*, *114*(13), 2491-2499.

**Alvarez-Erviti, L**., Rodriguez-Oroz, M. C., Cooper, J. M., Caballero, C., Ferrer, I., Obeso, J. A., & Schapira, A. H. (2010). Chaperone-mediated autophagy markers in Parkinson disease brains. *Archives of neurology*, *67*(12), 1464-1472.

**Alvarez-Erviti, L.,** Seow, Y., Schapira, A. H., Rodriguez-Oroz, M. C., Obeso, J. A., & Cooper, J. M. (2013). Influence of microRNA deregulation on chaperone-mediated autophagy and α-synuclein pathology in Parkinson's disease. *Cell death & disease*, *4*(3), e545.

**Anguiano, J.,** Garner, T. P., Mahalingam, M., Das, B. C., Gavathiotis, E., & Cuervo, A. M. (2013). Chemical modulation of chaperone-mediated autophagy by retinoic acid derivatives. *Nature chemical biology*, *9*(6), 374.

**Arranz, A. M.,** Delbroek, L., Van Kolen, K., Guimarães, M. R., Mandemakers, W., Daneels, G., ... & De Bock, P. J. (2015). LRRK2 functions in synaptic vesicle endocytosis through a kinase-dependent mechanism. *J Cell Sci*, *128*(3), 541-552.

**Baba, M.,** Takeshige, K., Baba, N., & Ohsumi, Y. (1994). Ultrastructural analysis of the autophagic process in yeast: detection of autophagosomes and their characterization. *The Journal of cell biology*, *124*(6), 903-913.

**Bandyopadhyay, U.,** Sridhar, S., Kaushik, S., Kiffin, R., & Cuervo, A. M. (2010). Identification of regulators of chaperone-mediated autophagy. *Molecular cell*, *39*(4), 535-547.

**Beach, T. G.,** Adler, C. H., Sue, L. I., Vedders, L., Lue, L., White III, C. L., ... & Walker, D. G. (2010). Multi-organ distribution of phosphorylated α-synuclein histopathology in subjects with Lewy body disorders. *Acta neuropathologica*, *119*(6), 689-702.

**Biesemann, C.,** Grønborg, M., Luquet, E., Wichert, S. P., Bernard, V., Bungers, S. R., ... & Urlaub, H. (2014). Proteomic screening of glutamatergic mouse brain synaptosomes isolated by fluorescence activated sorting. *The EMBO journal*, *33*(2), 157-170.

**Binotti, B.,** Pavlos, N. J., Riedel, D., Wenzel, D., Vorbrüggen, G., Schalk, A. M., ... & Chua, J. J. (2015). The GTPase Rab26 links synaptic vesicles to the autophagy pathway. *Elife*, *4*, e05597.

**Boland, B.,** Kumar, A., Lee, S., Platt, F. M., Wegiel, J., Yu, W. H., & Nixon, R. A. (2008). Autophagy induction and autophagosome clearance in neurons: relationship to autophagic pathology in Alzheimer's disease. *Journal of Neuroscience*, *28*(27), 6926-6937.

**Burke, R. E.,** & O'malley, K. (2013). Axon degeneration in Parkinson's disease. *Experimental neurology*, *246*, 72-83.

Button, R. W., Luo, S., & Rubinsztein, D. C. (2015). Autophagic activity in neuronal cell death. *Neuroscience bulletin*, *31*(4), 382-394.

**Cheng, H. C.,** Kim, S. R., Oo, T. F., Kareva, T., Yarygina, O., Rzhetskaya, M., ... & Komatsu, M. (2011). Akt suppresses retrograde degeneration of dopaminergic axons by inhibition of macroautophagy. *Journal of Neuroscience*, *31*(6), 2125-2135.

**Cheng, H. C**., Ulane, C. M., & Burke, R. E. (2010). Clinical progression in Parkinson disease and the neurobiology of axons. *Annals of neurology*, *67*(6), 715-725.

**Cheng, X. T.,** Zhou, B., Lin, M. Y., Cai, Q., & Sheng, Z. H. (2015). Axonal autophagosomes recruit dynein for retrograde transport through fusion with late endosomes. *J Cell Biol*, *209*(3), 377-386.

**Cherra, S. J.,** Kulich, S. M., Uechi, G., Balasubramani, M., Mountzouris, J., Day, B. W., & Chu, C. T. (2010). Regulation of the autophagy protein LC3 by phosphorylation. *The Journal of cell biology*, *190*(4), 533-539.

**Chiang, H. L.,** & Dice, J. F. (1988). Peptide sequences that target proteins for enhanced degradation during serum withdrawal. *Journal of Biological Chemistry*, *263*(14), 6797-6805.

**Chiang, H. L.,** Plant, C. P., & Dice, J. F. (1989). A role for a 70-kilodalton heat shock protein in lysosomal degradation of intracellular proteins. *Science*, *246*(4928), 382-385.

**Chu, Y.,** Dodiya, H., Aebischer, P., Olanow, C. W., & Kordower, J. H. (2009). Alterations in lysosomal and proteasomal markers in Parkinson's disease: relationship to alpha-synuclein inclusions. *Neurobiology of disease*, *35*(3), 385-398.

**Ciechanover, A.,** & Kwon, Y. T. (2015). Degradation of misfolded proteins in neurodegenerative diseases: therapeutic targets and strategies. *Experimental & molecular medicine*, *47*(3), e147.

**Clayton, D. F.,** & George, J. M. (1998). The synucleins: a family of proteins involved in synaptic function, plasticity, neurodegeneration and disease. *Trends in neurosciences*, *21*(6), 249-254.

**Clayton, D. F**., & George, J. M. (1999). Synucleins in synaptic plasticity and neurodegenerative disorders. *Journal of neuroscience research*, *58*(1), 120-129.

**Coleman, M. P.,** & Perry, V. H. (2002). Axon pathology in neurological disease: a neglected therapeutic target. *Trends in neurosciences*, *25*(10), 532-537.

**Conway, K. A.,** Harper, J. D., & Lansbury, P. T. (1998). Accelerated in vitro fibril formation by a mutant α-synuclein linked to early-onset Parkinson disease. *Nature medicine*, *4*(11), 1318.

**Crews, L.,** Spencer, B., Desplats, P., Patrick, C., Paulino, A., Rockenstein, E., ... & Masliah, E. (2010). Selective molecular alterations in the autophagy pathway in patients with Lewy body disease and in models of α-synucleinopathy. *PloS one*, *5*(2), e9313.

**Cuervo, A. M.,** & Dice, J. F. (1996). A receptor for the selective uptake and degradation of proteins by lysosomes. *Science*, *273*(5274), 501-503.

**Cuervo, A. M.,** & Dice, J. F. (2000). Regulation of lamp2a levels in the lysosomal membrane. *Traffic*, *1*(7), 570-583.

**Cuervo, A. M.,** & Dice, J. F. (2000). Unique properties of lamp2a compared to other lamp2 isoforms. *Journal of cell science*, *113*(24), 4441-4450.

**Cuervo, A. M.,** Hildebrand, H., Bomhard, E. M., & Dice, J. F. (1999). Direct lysosomal uptake of α2-microglobulin contributes to chemically induced nephropathy. *Kidney international*, *55*(2), 529-545.

**Cuervo, A. M.,** Hildebrand, H., Bomhard, E. M., & Dice, J. F. (1999). Direct lysosomal uptake of α2-microglobulin contributes to chemically induced nephropathy. *Kidney international*, *55*(2), 529-545.

**Cuervo, A. M.,** Knecht, E. R. W. I. N., Terlecky, S. R., & Dice, J. F. (1995). Activation of a selective pathway of lysosomal proteolysis in rat liver by prolonged starvation. *American Journal of Physiology-Cell Physiology*, *269*(5), C1200-C1208.

**Cuervo, A. M.,** Stefanis, L., Fredenburg, R., Lansbury, P. T., & Sulzer, D. (2004). Impaired degradation of mutant α-synuclein by chaperone-mediated autophagy. *Science*, *305*(5688), 1292-1295.

**Dehay** B.*,* Bove J.*,* Rodriguez-Muela N.*,* Perier C.*,* Recasens A.*,* Boya P. & Vila M. (2010*)* Pathogenic lysosomal depletion in Parkinson's disease. *J. Neurosci. 30,* 12535–12544

**Denker, A.,** Kröhnert, K., Bückers, J., Neher, E., & Rizzoli, S. O. (2011). The reserve pool of synaptic vesicles acts as a buffer for proteins involved in synaptic vesicle recycling. *Proceedings of the National Academy of Sciences*, 201112690.

**Dice, J. F.** (1990). Peptide sequences that target cytosolic proteins for lysosomal proteolysis. *Trends in biochemical sciences*, *15*(8), 305-309.

**Dice, J. F.,** Terlecky, S. R., Chiang, H. L., Olson, T. S., Isenman, L. D., Short-Russell, S. R., ... & Terlecky, L. J. (1990, December). A selective pathway for degradation of cytosolic proteins by lysosomes. In *Seminars in cell biology* (Vol. 1, No. 6, pp. 449-455).

**Dohi, E.,** Tanaka, S., Seki, T., Miyagi, T., Hide, I., Takahashi, T., ... & Sakai, N. (2012). Hypoxic stress activates chaperone-mediated autophagy and modulates neuronal cell survival. *Neurochemistry international*, *60*(4), 431-442.

**Forno, L. S.** (1996). Neuropathology of Parkinson's disease. *Journal of Neuropathology & Experimental Neurology*, *55*(3), 259-272.

**Fuhrmann, M.,** Mitteregger, G., Kretzschmar, H., & Herms, J. (2007). Dendritic pathology in prion disease starts at the synaptic spine. *Journal of Neuroscience*, *27*(23), 6224-6233.

**Gai, W. P.,** Power, J. H. T., Blumbergs, P. C., & Blessing, W. W. (1998). Multiple-system atrophy: a new α-synuclein disease?. *The Lancet*, *352*(9127), 547-548.

**Gao, L.,** She, H., Li, W., Zeng, J., Zhu, J., Jones, D. P., ... & Yang, Q. (2014). Oxidation of survival factor MEF2D in neuronal death and Parkinson's disease. *Antioxidants & redox signaling*, *20*(18), 2936-2948.

**Gelpi, E**., Navarro-Otano, J., Tolosa, E., Gaig, C., Compta, Y., Rey, M. J., ... & Ribalta, T. (2014). Multiple organ involvement by alpha-synuclein pathology in Lewy body disorders. *Movement Disorders*, *29*(8), 1010-1018.

**Gough, N.R.,** Hatem, C.L., & Fambrough, D.M. (1995). The family of LAMP-2 proteins arises by alternative splicing from a single gene: characterization of the avian LAMP-2 gene and identification of mammalian homologs of LAMP-2b and LAMP-2c. *DNA and cell biology*, *14*(10), 863-867.

**Gouras, G.** K., Tampellini, D., Takahashi, R. H., & Capetillo-Zarate, E. (2010). Intraneuronal β-amyloid accumulation and synapse pathology in Alzheimer's disease. *Acta neuropathologica*, *119*(5), 523-541.

**Hara, T.,** Nakamura, K., Matsui, M., Yamamoto, A., Nakahara, Y., Suzuki-Migishima, R., ... & Mizushima, N. (2006). Suppression of basal autophagy in neural cells causes neurodegenerative disease in mice. *Nature*, *441*(7095), 885.

Hernandez, D., Torres, C. A., Setlik, W., Cebrián, C., Mosharov, E. V., Tang, G., ... & **Gershon, M.** (2012). Regulation of presynaptic neurotransmission by macroautophagy. *Neuron*, *74*(2), 277-284.

**Hollenbeck, P. J.** (1993). Products of endocytosis and autophagy are retrieved from axons by regulated retrograde organelle transport. *The Journal of cell biology*, *121*(2), 305-315.

**Holtzman, E.** (1971). Cytochemical studies of protein transport in the nervous system. *Phil. Trans. R. Soc. Lond. B*, *261*(839), 407-421.

**Inoue, K.,** Rispoli, J., Yang, L., MacLeod, D., Beal, M. F., Klann, E., & Abeliovich, A. (2013). Coordinate regulation of mature dopaminergic axon morphology by macroautophagy and the PTEN signaling pathway. *PLoS genetics*, *9*(10), e1003845.

**Iwai, A.,** Yoshimoto, M., Masliah, E., & Saitoh, T. (1995). Non-A. beta. Component of Alzheimer's Disease Amyloid (NAC) is Amyloidogenic. *Biochemistry*, *34*(32), 10139-10145.

**Kabeya, Y.,** Mizushima, N., Ueno, T., Yamamoto, A., Kirisako, T., Noda, T., ... & Yoshimori, T. (2000). LC3, a mammalian homologue of yeast Apg8p, is localized in autophagosome membranes after processing. *The EMBO journal*, *19*(21), 5720-5728.

**Kaushik, S**., & Cuervo, A. M. (2012). Chaperone-mediated autophagy: a unique way to enter the lysosome world. *Trends in cell biology*, *22*(8), 407-417.

**Kaushik, S.,** Massey, A. C., Mizushima, N., & Cuervo, A. M. (2008). Constitutive activation of chaperone-mediated autophagy in cells with impaired macroautophagy. *Molecular biology of the cell*, *19*(5), 2179-2192.

**Kiffin, R**., Christian, C., Knecht, E., & Cuervo, A. M. (2004). Activation of chaperone-mediated autophagy during oxidative stress. *Molecular biology of the cell*, *15*(11), 4829-4840.

**Kim, J.,** Kundu, M., Viollet, B., & Guan, K. L. (2011). AMPK and mTOR regulate autophagy through direct phosphorylation of Ulk1. *Nature cell biology*, *13*(2), 132.

Kiriyama, Y., & Nochi, H. (2015). The function of autophagy in neurodegenerative diseases. *International journal of molecular sciences*, *16*(11), 26797-26812.

**Klionsky, D. J.,** Abdelmohsen, K., Abe, A., Abedin, M. J., Abeliovich, H., Acevedo Arozena, A., ... & Adhihetty, P. J. (2016). Guidelines for the use and interpretation of assays for monitoring autophagy. *Autophagy*, *12*(1), 1-222.

**Klionsky, D. J.,** Cregg, J. M., Dunn, W. A., Emr, S. D., Sakai, Y., Sandoval, I. V., ... & Ohsumi, Y. (2003). A unified nomenclature for yeast autophagy-related genes. *Developmental cell*, *5*(4), 539-545.

**Koga, H**., Martinez-Vicente, M., Arias, E., Kaushik, S., Sulzer, D., & Cuervo, A. M. (2011). Constitutive upregulation of chaperone-mediated autophagy in Huntington's disease. *Journal of Neuroscience*, *31*(50), 18492-18505.

**Komatsu, M.,** Waguri, S., Chiba, T., Murata, S., Iwata, J. I., Tanida, I., ... & Tanaka, K. (2006). Loss of autophagy in the central nervous system causes neurodegeneration in mice. *Nature*, *441*(7095), 880.

**Komatsu, M**., Wang, Q. J., Holstein, G. R., Friedrich, V. L., Iwata, J. I., Kominami, E., ... & Yue, Z. (2007). Essential role for autophagy protein Atg7 in the maintenance of axonal homeostasis and the prevention of axonal degeneration. *Proceedings of the National Academy of Sciences*, *104*(36), 14489-14494.

**Kroemer, G**., & Levine, B. (2008). Autophagic cell death: the story of a misnomer. *Nature reviews Molecular cell biology*, *9*(12), 1004.

**Larsen, K. E.,** Fon, E. A., Hastings, T. G., Edwards, R. H., & Sulzer, D. (2002). Methamphetamine-induced degeneration of dopaminergic neurons involves autophagy and upregulation of dopamine synthesis. *Journal of Neuroscience*, *22*(20), 8951-8960.

**Lee, J. A.,** & Gao, F. B. (2009). Inhibition of autophagy induction delays neuronal cell loss caused by dysfunctional ESCRT-III in frontotemporal dementia. *Journal of Neuroscience*, *29*(26), 8506-8511.

**Lewy, F.** H. (1912). Paralysis agitans. I. *Pathologische anatomie. Handbuch der neurologie*.

**Liberski, P. P.,** Sikorska, B., Gibson, P., & Brown, P. (2011). Autophagy contributes to widespread neuronal degeneration in hamsters infected with the Echigo-1 strain of Creutzfeldt-Jakob disease and mice infected with the Fujisaki strain of Gerstmann-Sträussler-Scheinker (GSS) syndrome. *Ultrastructural pathology*, *35*(1), 31-36.

**Lv, L.,** Li, D., Zhao, D., Lin, R., Chu, Y., Zhang, H., ... & Wang, G. (2011). Acetylation targets the M2 isoform of pyruvate kinase for degradation through chaperone-mediated autophagy and promotes tumor growth. *Molecular cell*, *42*(6), 719-730.

**Maday, S. (2016).** Mechanisms of neuronal homeostasis: Autophagy in the axon. *Brain research*, *1649*, 143-150.

**Maday, S.,** & Holzbaur, E. L. (2014). Autophagosome biogenesis in primary neurons follows an ordered and spatially regulated pathway. *Developmental cell*, *30*(1), 71-85.

**Mak, S. K.,** McCormack, A. L., Manning-Bog, A. B., Cuervo, A. M., & Di Monte, D. A. (2010). Lysosomal degradation of α-synuclein in vivo. *Journal of Biological Chemistry*, jbc-M109.

**Marin, C., & Aguilar, E.** (2011). In vivo 6-OHDA-induced neurodegeneration and nigral autophagic markers expression. *Neurochemistry international*, *58*(4), 521-526.

**Martinez-Vicente, M.,** Talloczy, Z., Kaushik, S., Massey, A. C., Mazzulli, J., Mosharov, E. V., ... & Dauer, W. (2008). Dopamine-modified α-synuclein blocks chaperone-mediated autophagy. *The Journal of clinical investigation*, *118*(2), 777-788.

**Marzella, L.,** Ahlberg, J., & Glaumann, H. (1981). Autophagy, heterophagy, microautophagy and crinophagy as the means for intracellular degradation. *Virchows Archiv B Cell Pathology Zell-pathologie*, *36*(1), 219-234..

**Massey, A. C.,** Kaushik, S., Sovak, G., Kiffin, R., & Cuervo, A. M. (2006). Consequences of the selective blockage of chaperone-mediated autophagy. *Proceedings of the National Academy of Sciences*, *103*(15), 5805-5810.

**Matta, S.,** Van Kolen, K., da Cunha, R., van den Bogaart, G., Mandemakers, W., Miskiewicz, K., ... & Delbroek, L. (2012). LRRK2 controls an EndoA phosphorylation cycle in synaptic endocytosis. *Neuron*, *75*(6), 1008-1021.

**Miner, L. H.,** Jedema, H. P., Moore, F. W., Blakely, R. D., Grace, A. A., & Sesack, S. R. (2006). Chronic stress increases the plasmalemmal distribution of the norepinephrine transporter and the coexpression of tyrosine hydroxylase in norepinephrine axons in the prefrontal cortex. *Journal of Neuroscience*, *26*(5), 1571-1578.

**Mizushima, N.,** Yoshimori, T., & Ohsumi, Y. (2011). The role of Atg proteins in autophagosome formation. *Annual review of cell and developmental biology*, *27*, 107-132.

**Murphy, K. E.,** Gysbers, A. M., Abbott, S. K., Spiro, A. S., Furuta, A., Cooper, A., ... & Halliday, G. M. (2015). Lysosomal-associated membrane protein 2 isoforms are differentially affected in early Parkinson's disease. *Movement Disorders*, *30*(12), 1639-1647.

**Murphy, K. E.,** Gysbers, A. M., Abbott, S. K., Tayebi, N., Kim, W. S., Sidransky, E., ... & Halliday, G. M. (2014). Reduced glucocerebrosidase is associated with increased α-synuclein in sporadic Parkinson's disease. *Brain*, *137*(3), 834-848.

**Nakatogawa, H.,** Suzuki, K., Kamada, Y., & Ohsumi, Y. (2009). Dynamics and diversity in autophagy mechanisms: lessons from yeast. *Nature reviews Molecular cell biology*, *10*(7), 458.

**Newell, K. L**., Boyer, P., Gomez-Tortosa, E., & Hobbs, W. (1999). Alpha-synuclein immunoreactivity is present in axonal swellings in neuroaxonal dystrophy and acute traumatic brain injury. *Journal of neuropathology and experimental neurology*, *58*(12), 1263.

**Nikoletopoulou, V.,** Sidiropoulou, K., Kallergi, E., Dalezios, Y., & Tavernarakis, N. (2017). Modulation of autophagy by BDNF underlies synaptic plasticity. *Cell metabolism*, *26*(1), 230-242.

**Nixon, R. A**., Wegiel, J., Kumar, A., Yu, W. H., Peterhoff, C., Cataldo, A., & Cuervo, A. M. (2005). Extensive involvement of autophagy in Alzheimer disease: an immuno-electron microscopy study. *Journal of Neuropathology & Experimental Neurology*, *64*(2), 113-122.

**Oddo, S.,** Caccamo, A., Shepherd, J. D., Murphy, M. P., Golde, T. E., Kayed, R., ... & LaFerla, F. M. (2003). Triple-transgenic model of Alzheimer's disease with plaques and tangles: intracellular Aβ and synaptic dysfunction. *Neuron*, *39*(3), 409-421.

**Okerlund, N. D.,** Schneider, K., Leal-Ortiz, S., Montenegro-Venegas, C., Kim, S. A., Garner, L. C., ... & Garner, C. C. (2017). Bassoon controls presynaptic autophagy through Atg5. *Neuron*, *93*(4), 897-913.

**Pang, S.,** Chen, D., Zhang, A., Qin, X., & Yan, B. (2012). Genetic analysis of the LAMP-2 gene promoter in patients with sporadic Parkinson's disease. *Neuroscience letters*, *526*(1), 63-67.

**Pankiv, S.,** Clausen, T. H., Lamark, T., Brech, A., Bruun, J. A., Outzen, H., ... & Johansen, T. (2007). p62/SQSTM1 binds directly to Atg8/LC3 to facilitate degradation of ubiquitinated protein aggregates by autophagy. *Journal of biological chemistry*.

**Papagiannakis, N**., Xilouri, M., Koros, C., Stamelou, M., Antonelou, R., Maniati, M., ... & Stefanis, L. (2015). Lysosomal alterations in peripheral blood mononuclear cells of Parkinson's disease patients. *Movement Disorders*, *30*(13), 1830-1834.

**Plowey, E. D.,** & Chu, C. T. (2011). Synaptic dysfunction in genetic models of Parkinson's disease: a role for autophagy?. *Neurobiology of disease*, *43*(1), 60-67.

**Plowey, E. D.,** Cherra III, S. J., Liu, Y. J., & Chu, C. T. (2008). Role of autophagy in G2019S-LRRK2-associated neurite shortening in differentiated SH-SY5Y cells. *Journal of neurochemistry*, *105*(3), 1048-1056.

**Raff, M. C.,** Whitmore, A. V., & Finn, J. T. (2002). Axonal self-destruction and neurodegeneration. *Science*, *296*(5569), 868-871.

**Ramonet, D**., Daher, J. P. L., Lin, B. M., Stafa, K., Kim, J., Banerjee, R., ... & Liu, Y. (2011). Dopaminergic neuronal loss, reduced neurite complexity and autophagic

abnormalities in transgenic mice expressing G2019S mutant LRRK2. *PloS one*, *6*(4), e18568.

**Ravikumar, B.,** Vacher, C., Berger, Z., Davies, J. E., Luo, S., Oroz, L. G., ... & Rubinsztein, D. C. (2004). Inhibition of mTOR induces autophagy and reduces toxicity of polyglutamine expansions in fly and mouse models of Huntington disease. *Nature genetics*, *36*(6), 585.

**Rodriguez-Navarro, J. A.,** Kaushik, S., Koga, H., Dall'Armi, C., Shui, G., Wenk, M. R., ... & Cuervo, A. M. (2012). Inhibitory effect of dietary lipids on chaperone-mediated autophagy. *Proceedings of the National Academy of Sciences*, *109*(12), E705-E714.

**Rothaug, M.,** Stroobants, S., Schweizer, M., Peters, J., Zunke, F., Allerding, M., ... & Blanz, J. (2015). LAMP-2 deficiency leads to hippocampal dysfunction but normal clearance of neuronal substrates of chaperone-mediated autophagy in a mouse model for Danon disease. *Acta neuropathologica communications*, *3*(1), 6.

**Rothenberg, C.,** Srinivasan, D., Mah, L., Kaushik, S., Peterhoff, C. M., Ugolino, J., ... & Monteiro, M. J. (2010). Ubiquilin functions in autophagy and is degraded by chaperone-mediated autophagy. *Human molecular genetics*, *19*(16), 3219-3232.

**Sacino, A. N.,** Brooks, M. M., Chakrabarty, P., Saha, K., Khoshbouei, H., Golde, T. E., & Giasson, B. I. (2017). Proteolysis of α-synuclein fibrils in the lysosomal pathway limits induction of inclusion pathology. *Journal of neurochemistry*, *140*(4), 662-678.

**Sahu, R.,** Kaushik, S., Clement, C. C., Cannizzo, E. S., Scharf, B., Follenzi, A., ... & Santambrogio, L. (2011). Microautophagy of cytosolic proteins by late endosomes. *Developmental cell*, *20*(1), 131-139.

**Sala, G.,** Arosio, A., Stefanoni, G., Melchionda, L., Riva, C., Marinig, D., ... & Ferrarese, C. (2013). Rotenone upregulates alpha-synuclein and myocyte enhancer factor 2D independently from lysosomal degradation inhibition. *BioMed research international*, *2013*.

**Sala, G.,** Stefanoni, G., Arosio, A., Riva, C., Melchionda, L., Saracchi, E., ... & Ferrarese, C. (2014). Reduced expression of the chaperone-mediated autophagy carrier hsc70 protein in lymphomonocytes of patients with Parkinson's disease. *Brain research*, *1546*, 46-52.

**Sanchez-Varo, R.,** Trujillo-Estrada, L., Sanchez-Mejias, E., Torres, M., Baglietto-Vargas, D., Moreno-Gonzalez, I., ... & Davila, J. C. (2012). Abnormal accumulation of autophagic vesicles correlates with axonal and synaptic pathology in young Alzheimer's mice hippocampus. *Acta neuropathologica*, *123*(1), 53-70.

**Schneider, J.** L., Suh, Y., & Cuervo, A. M. (2014). Deficient chaperone-mediated autophagy in liver leads to metabolic dysregulation. *Cell metabolism*, *20*(3), 417-432.

**Selkoe, D. J.** (2002). Alzheimer's disease is a synaptic failure. *Science*, *298*(5594), 789-791.

**Shehata, M**., Matsumura, H., Okubo-Suzuki, R., Ohkawa, N., & Inokuchi, K. (2012). Neuronal stimulation induces autophagy in hippocampal neurons that is involved in AMPA receptor degradation after chemical long-term depression. *Journal of Neuroscience*, *32*(30), 10413-10422.

**Sikorska, B**., Liberski, P. P., Giraud, P., Kopp, N., & Brown, P. (2004). Autophagy is a part of ultrastructural synaptic pathology in Creutzfeldt–Jakob disease: a brain biopsy study. *The international journal of biochemistry & cell biology*, *36*(12), 2563-2573.

**Soukup, S**. F., Kuenen, S., Vanhauwaert, R., Manetsberger, J., Hernández-Díaz, S., Swerts, J., ... & Geens, A. (2016). A LRRK2-dependent endophilina phosphoswitch is critical for macroautophagy at presynaptic terminals. *Neuron*, *92*(4), 829-844.

**Spillantini,** M. G., Schmidt, M. L., Lee, V. M. Y., Trojanowski, J. Q., Jakes, R., & Goedert, M. (1997). α-Synuclein in Lewy bodies. *Nature*, *388*(6645), 839.

**Stefanis, L.,** Larsen, K. E., Rideout, H. J., Sulzer, D., & Greene, L. A. (2001). Expression of A53T mutant but not wild-type α-synuclein in PC12 cells induces alterations of the ubiquitin-dependent degradation system, loss of dopamine release, and autophagic cell death. *Journal of Neuroscience*, *21*(24), 9549-9560.

**Tagliaferro, P.,** & Burke, R. E. (2016). Retrograde axonal degeneration in Parkinson disease. *Journal of Parkinson's disease*, *6*(1), 1-15.

**Tammineni, P.,** Ye, X., Feng, T., Aikal, D., & Cai, Q. (2017). Impaired retrograde transport of axonal autophagosomes contributes to autophagic stress in Alzheimer's disease neurons. *Elife*, *6*, e21776.

**Tanaka, Y.,** Guhde, G., Suter, A., Eskelinen, E. L., Hartmann, D., Lüllmann-Rauch, R., ... & Saftig, P. (2000). Accumulation of autophagic vacuoles and cardiomyopathy in LAMP-2-deficient mice. *Nature*, *406*(6798), 902.

**Tanida, I.,** Minematsu-Ikeguchi, N., Ueno, T., & Kominami, E. (2005). Lysosomal turnover, but not a cellular level, of endogenous LC3 is a marker for autophagy. *Autophagy*, *1*(2), 84-91.

**Tanik, S**. A., Schultheiss, C. E., Volpicelli-Daley, L. A., Brunden, K. R., & Lee, V. M. (2013). Lewy body-like α-synuclein aggregates resist degradation and impair macroautophagy. *Journal of Biological Chemistry*, *288*(21), 15194-15210.

**Thompson, L**. M., Aiken, C. T., Kaltenbach, L. S., Agrawal, N., Illes, K., Khoshnan, A., ... & Lukacsovich, T. (2009). IKK phosphorylates Huntingtin and targets it for degradation by the proteasome and lysosome. *The Journal of cell biology*, *187*(7), 1083-1099.

**Tooze, S. A**., & Yoshimori, T. (2010). The origin of the autophagosomal membrane. *Nature cell biology*, *12*(9), 831.

**Trinh, J.,** Amouri, R., Duda, J. E., Morley, J. F., Read, M., Donald, A., ... & Sassi, S. B. (2014). A comparative study of Parkinson's disease and leucine-rich repeat kinase 2 p. G2019S parkinsonism. *Neurobiology of aging*, *35*(5), 1125-1131.

**Uytterhoeven, V**., Kuenen, S., Kasprowicz, J., Miskiewicz, K., & Verstreken, P. (2011). Loss of skywalker reveals synaptic endosomes as sorting stations for synaptic vesicle proteins. *Cell*, *145*(1), 117-132.

**Vogiatzi, T**., Xilouri, M., Vekrellis, K., & Stefanis, L. (2008). Wild type a-synuclein is degraded by chaperone mediated autophagy and macroautophagy in neuronal cells. *Journal of Biological Chemistry*.

**Wang, C.,** Wang, H., Zhang, D., Luo, W., Liu, R., Xu, D., ... & Liu, Z. (2018). Phosphorylation of ULK1 affects autophagosome fusion and links chaperone-mediated autophagy to macroautophagy. *Nature communications*, *9*(1), 3492.
**Wang, Q. J.,** Ding, Y., Kohtz, S., Mizushima, N., Cristea, I. M., Rout, M. P., ... & Yue, Z. (2006). Induction of autophagy in axonal dystrophy and degeneration. *Journal of Neuroscience*, *26*(31), 8057-8068.

**Webb, J. L.,** Ravikumar, B., Atkins, J., Skepper, J. N., & Rubinsztein, D. C. (2003). α-Synuclein is degraded by both autophagy and the proteasome. *Journal of Biological Chemistry*, *278*(27), 25009-25013.

**Wing, S. S.,** Chiang, H. L., Goldberg, A. L., & Dice, J. F. (1991). Proteins containing peptide sequences related to Lys-Phe-Glu-Arg-Gln are selectively depleted in liver and heart, but not skeletal muscle, of fasted rats. *Biochemical Journal*, *275*(1), 165-169.

**Wu, G.,** Wang, X., Feng, X., Zhang, A., Li, J., Gu, K., ... & Yan, B. (2011). Altered expression of autophagic genes in the peripheral leukocytes of patients with sporadic Parkinson's disease. *Brain research*, *1394*, 105-111.

**Xilouri, M.,** Brekk, O. R., Landeck, N., Pitychoutis, P. M., Papasilekas, T., Papadopoulou-Daifoti, Z., Kirik, D., & Stefanis, L. (2013). Boosting chaperone-mediated autophagy in vivo mitigates α-synuclein-induced neurodegeneration. *Brain*, *136*(7), 2130-2146.

**Xilouri, M.,** Brekk, O. R., Polissidis, A., Chrysanthou-Piterou, M., Kloukina, I., & Stefanis, L. (2016). Impairment of chaperone-mediated autophagy induces dopaminergic neurodegeneration in rats. *Autophagy*, *12*(11), 2230-2247.

**Xilouri, M.,** Vogiatzi, T., Vekrellis, K., Park, D., & Stefanis, L. (2009). Abberant α-synuclein confers toxicity to neurons in part through inhibition of chaperone-mediated autophagy. *PloS one*, *4*(5), e5515.

**Yang, Q**., She, H., Gearing, M., Colla, E., Lee, M., Shacka, J. J., & Mao, Z. (2009). Regulation of neuronal survival factor MEF2D by chaperone-mediated autophagy. *Science*, *323*(5910), 124-127.

**Yang, Y.,** Fukui, K., Koike, T., & Zheng, X. (2007). Induction of autophagy in neurite degeneration of mouse superior cervical ganglion neurons. *European Journal of Neuroscience*, *26*(10), 2979-2988.

**Yu, W.** H., Cuervo, A. M., Kumar, A., Peterhoff, C. M., Schmidt, S. D., Lee, J. H., ... & Jiang, Y. (2005). Macroautophagy—a novel β-amyloid peptide-generating pathway activated in Alzheimer's disease. *J Cell Biol*, *171*(1), 87-98.

**Zhang, C.,** & Cuervo, A. M. (2008). Restoration of chaperone-mediated autophagy in aging liver improves cellular maintenance and hepatic function. *Nature medicine*, *14*(9), 959.

## G. List of Abbreviations

AD: Alzheimer's Disease

ALS: Amyotrophic Lateral Sclerosis

Atg: autophagy-related genes

CMA: chaperone-mediated autophagy

CMA: Chaperone-Mediated Autophagy

DA: dopamine

DAT: dopamine transporter

EM: electron microscopy

GFAP: glial fibrillary acidic protein

GFP: green fluorescent protein

HD: Huntington's Disease

Hsc70: heat shock protein of 70 kDa

IBA-1: ionized calcium-binding adapter molecule 1

LAMP2A: lysosomal associated membrane protein 2A

Lamp-2A: Lysosome-associated membrane protein 2

LE: late endosomes

LIR: LC3-interacting region

LRRK2: Leucine-rich repeat kinase 2

mTOR: mammalian target of rapamycin

MVB: multivesicular bodies

p62 or SQSTM1: sequestosome

PBS: Phosphate-buffered saline

PD: Parkinson's disease

PE: Phosphatidylethanolamine

PI3K: Phosphatidyl Inositol 3 Kinase

PLCγ: Phosphoinositide phospholipase Cγ

PtdIns3: Phosphatidylinositol 3,5-bisphosphate

rAAV: recombinant adeno-associated virus

shRNA: short hairpin RNA

SN: substantia nigra

SNpc: substantia nigra pars compact

TH: tyrosine hydroxylase

UBLs: ubiquitin-like proteins

ULK1: unc-51-like kinase 1